

Data Acquisition System for Exoskeletons



Author

HINNA NAYAB

00000171882

Supervisor

Dr. Umar Ansari

DEPARTMENT OF BIOMEDICAL ENGINEERING AND SCIENCES
SCHOOL OF MECHANICAL & MANUFACTURING ENGINEERING
NATIONAL UNIVERSITY OF SCIENCES AND TECHNOLOGY

ISLAMABAD, PAKISTAN

FEBRUARY, 2019

Data Acquisition System for Exoskeletons

Author

HINNA NAYAB

00000171882

A thesis submitted in partial fulfillment of the requirements for the degree of
MS Biomedical Engineering

Thesis Supervisor:

Dr. Umar Ansari

Thesis Supervisor's Signature: _____

DEPARTMENT OF BIOMEDICAL ENGINEERING AND SCIENCES
SCHOOL OF MECHANICAL & MANUFACTURING ENGINEERING
NATIONAL UNIVERSITY OF SCIENCES AND TECHNOLOGY,
ISLAMABAD, PAKISTAN
FEBRUARY, 2019

THESIS ACCEPTANCE CERTIFICATE

It is certified that the final copy of MS Thesis written by NS Hinna Nayab (Registration No. 00000171882), of SMME (School of Mechanical and Manufacturing Engineering) has been vetted by undersigned, found complete in all respects as per NUST statutes / regulations, is free of plagiarism, errors and mistakes and is accepted as partial fulfillment for award of MS/MPhil Degree. It is further certified that necessary amendments as pointed out by GEC members of the scholar have also been incorporated in the thesis.

Signature: _____

Name of Supervisor: Dr. Umar Ansari

Date: _____

Signature (HOD): _____

Date: _____

Signature (Principal): _____

Date: _____

Declaration

I certify that this research work titled “*Data Acquisition System for Exoskeletons*” is my own work. The work has not been presented elsewhere for assessment. The material that has been used from other sources it has been properly acknowledged / referred.

Signature of Student

HINNA NAYAB

00000171882

Plagiarism Certificate (Turnitin Report)

This thesis has been checked for Plagiarism. Turnitin report endorsed by Supervisor is attached.

Signature of Student

HINNA NAYAB

00000171882

Signature of Supervisor

Copyright Statement

- Copyright in text of this thesis rests with the student author. Copies (by any process) either in full, or of extracts, may be made only in accordance with instructions given by the author and lodged in the Library of NUST School of Mechanical & Manufacturing Engineering (SMME). Details may be obtained by the Librarian. This page must form part of any such copies made. Further copies (by any process) may not be made without the permission (in writing) of the author.
- The ownership of any intellectual property rights which may be described in this thesis is vested in NUST School of Mechanical & Manufacturing Engineering, subject to any prior agreement to the contrary, and may not be made available for use by third parties without the written permission of the SMME, which will prescribe the terms and conditions of any such agreement.
- Further information on the conditions under which disclosures and exploitation may take place is available from the Library of NUST School of Mechanical & Manufacturing Engineering, Islamabad.

ACKNOWLEDGEMENTS

I am extremely thankful to Almighty ALLAH for enabling me to take on the task of completing my Master's Research. Had HE not helped me throughout the process, I could not have done it by myself.

I would also like to express my sincerest gratitude to my project supervisor, Dr. Umar Ansari for his guidance, support and motivation; and for helping me along the course of the research wherever I felt stuck. I am also obliged to Dr. Nousheen Fatima (HoD BMES) and Dr. Nabeel Anwar for their valuable advices and administrative support.

I would like to say Thank you to my friend Palwasha Kifayat for sticking by my side during hard times and would also like to thank Maleeha Asad, Mahnoor Malik, Sadia Bhatti, Fatima Ehsan, Sundus Shah, Anisa Tahir and Musawira Iftikhar for making it all easy for me in the tough phase.

Sincerest thanks to my friends Maleeha, Fatima, Palwasha and Musawira who participated as subjects in the experiments of this research. Thank you to everyone who was a support emotionally and professionally.

Last but not the least; I am always immensely grateful to my wonderful parents who are a pillar of support and strength for me. Thank you for believing in me and putting your trust in me during all my endeavours. My siblings, Tahira, Mehwish, Basit and Zarrar play an important role in making higher studies and particularly Masters Research easy for me. I could not end this without mentioning my best friend whose support and words of encouragement mean the world to me.

*Dedicated to the ones that are lost but haven't given up and are still
trying to figure out their ways into life*

TABLE OF CONTENTS

CHAPTER 1	1
INTRODUCTION	1
1.1 EXOSKELETON	1
1.2 DATA ACQUISTION	2
1.3 DAQ TECHNIQUES	2
1.4 OBJECTIVES OF THIS RESEARCH	3
CHAPTER 2	4
LITERATURE REVIEW	4
CHAPTER 3	12
METHODOLOGY	12
3.1 YAW PITCH ROLL	12
3.2 SPINAL CURVES	13
3.2.1 VERTEBRAE	13
3.2.2 CERVICAL, THORACIC AND LUMBAR SPINE	14
3.3 INERTIAL NAVIGATION SYSTEM	15
3.3.1 ACCELEROMETER OF THE IMU	15
3.3.2 GYROMETER OF THE IMU	16
3.4 INITIAL PATHWAY TAKEN FOR PROJECT	17
(IMU DISTANCE APPROACH)	17
3.5 EXPERIEMENTS PERFORMED WITH ACCELEROMETER	17
3.6 GYROMETER BASED APPROACH	18
3.7 PORTBALE DEVICE	20
CHAPTER 4	21
SYSTEM DEVELOPMENT	21
4.1 INERTIAL MEASUREMENT UNIT (MPU6050)	21
4.1.1 DIGITAL MOTION PROCESSOR	21
4.1.2 PIN CONNECTIONS OF MPU6050 WITH ESP8266	22
4.2 ESP-8266 Wi-Fi Based MCU	24
4.3 TCA9548A I2C Multiplexer	25

CHAPTER 5	28
EXPERIMENTATION AND RESULTS	28
5.1 CALIBRATION.....	28
5.2 APPLICATIONS OF THE DAQ SYSTEM	29
5.2.1 BIOMECHANICS OF THE SPINE	29
5.2.1.1 SITTING POSITION	31
5.2.1.1.1 CERVICAL REGION	31
5.2.1.1.2 THORACIC REGION	32
5.2.1.1.3 LUMBAR REGION	33
5.2.1.2 LYING DOWN POSITION	33
5.2.1.2.1 CERVIAL REGION	34
5.2.1.2.2 THORACIC REGION	34
5.2.1.2.3 LUMBAR REGION	35
5.2.2 COMBINED GRAPHS.....	36
5.2.2.1 ORIENTATION DATA OF SPINE DURING SITTING	36
5.2.2.2 ORIENTATION DATA OF SPINE DURING LYING DOWN	37
5.2.3 COMPARISON OF VALUES WITH MOTION PROCESSING SOFTWARE	38
5.2.4 ACCUMULATED SUBJECTS' DATA.....	39
5.2.5 BIOMECHANICS OF THE WRIST JOINT.....	40
5.2.5.1 WRIST JOINT.....	40
5.2.5.2 ANALYZING THE DATA & RESULTS	41
5.2.5.2.1 EXTENSION	41
5.2.5.2.2 FLEXION.....	42
5.2.5.2.3 RADIAL FLEXION (LEFT MOVEMENT)	43
5.2.5.2.4 ULNAR FLEXION (RIGHT MOVEMENT)	43
5.2.5.3 Accumulated Subjects' Data	44
CHAPTER 6	45
CONCLUSION AND FUTURE PROSPECTS	45
6.1 FUTURE PROSPECTS	46
REFERENCES	47
APPENDIX A	50
ARDUINO CODE:.....	50

APPENDIX B	56
MATLAB CODE:	56
PLAGIARISM REPORT	60

LIST OF FIGURES

FIGURE 1 SUBJECT WITH THE POSTURE MONITORING SYSTEM (7).....	4
FIGURE 2 FIBER OPTIC AND VIDEO SYSTEM ATTACHMENT (9).....	5
FIGURE 3 SPINE STRESS MONITORING SYSTEM WORN BY PATIENT (10)	6
FIGURE 4 MRI COMPATIBLE CHAIR TO STUDY POSTURE DURING DIFFERENT SITTING POSITIONS (11)	6
FIGURE 5 FORMETRIC 4D DEVICE (12)	7
FIGURE 6 THE MECHANICAL STRUCTURE DIAGRAM OF ROBOTIC EXOSKELETON (14).....	7
FIGURE 7 THE TRIANGULATION MEASUREMENT SCHEME (15).....	8
FIGURE 8 SENSOR SETUP ATTACHED TO THE PATIENT (19).....	9
FIGURE 9 WEARABLE SPINE MONITORING SYSTEM WITH FLEXIBLE STRAPS (21).....	10
FIGURE 10 VIRTUAL REALITY 6 DEGREES OF FREEDOM EXPERIMENTAL SETUP (22).....	10
FIGURE 11 ROTATIONS IN FRAMES: EULER ANGLES	12
FIGURE 12 SPINAL CURVES.....	14
FIGURE 13 INERTIAL MEASUREMENT UNIT.....	15
FIGURE 14 ANGLES FROM A GYROSCOPE.....	16
FIGURE 15 FINDING DISTANCE USING ACCELEROMETER OF THE IMU.....	18
FIGURE 16 YAW, PITCH, ROLL VALUES FROM GYROMETER OF THE IMU	19
FIGURE 17 MPU6050 MOTION SENSOR (24)	21
FIGURE 18 MPU 6000 FAMILY BLOCK DIAGRAM.....	22
FIGURE 19 WIRING DIAGRAM OF MPU6050 WITH WEMOS D1 MINI	23

FIGURE 20 ESP8266 WEMOS D1 MINI	25
FIGURE 21 TCA9548A MULTIPLEXER.....	26
FIGURE 22 APPLICATION DIAGRAM OF TCA9548A MULTIPLEXER	27
FIGURE 23 SETUP FOR THE EXPERIMENT ON SPINE	30
FIGURE 24 PLANES OF HUMAN BODY ROTATIONS.....	30
FIGURE 25 ORIENTATION DURING SITTING POSITION.....	31
FIGURE 26 ANGULAR DATA OF CERVICAL REGION IN SITTING POSITION.....	32
FIGURE 27 ANGULAR DATA OF THORACIC REGION IN SITTING POSITION.....	32
FIGURE 28 ANGULAR DATA OF LUMBAR REGION IN SITTING POSITION	33
FIGURE 29 ANGULAR DATA OF CERVICAL REGION IN LYING DOWN POSITION	34
FIGURE 30 ANGULAR DATA OF THORACIC REGION IN LYING DOWN POSITION	35
FIGURE 31 ANGULAR DATA OF LUMBAR REGION IN LYING DOWN POSITION	35
FIGURE 32 COMBINED ANGULAR DATA OF SPINE DURING SITTING	36
FIGURE 33 COMBINED ANGULAR DATA OF SPINE DURING LYING DOWN POSITION	37
FIGURE 34 CHANGE IN ORIENTATION DURING TRANSITION FROM LYING DOWN TO SITTING	38
FIGURE 35 SIDE PROFILE OF THE SUBJECT TO ANALYZE WITH KINOVEA	39
FIGURE 36 MOVEMENTS OF THE WRIST JOINT (27).....	40
FIGURE 37 SETUP TO TEST DAQ SYSTEM ON WRIST JOINT MOTION.....	41
FIGURE 38 EXTENSION OF WRIST JOINT	42
FIGURE 39 FLEXION OF THE WRIST JOINT	42
FIGURE 40 RADIAL FLEXION OF THE WRIST JOINT.....	43
FIGURE 41 ULNAR FLEXION OF THE WRIST JOINT	44

LIST OF TABLES

TABLE 1 PIN CONNECTIONS OF MPU6050 WITH ESP8266.....	22
TABLE 2 TECHNICAL SPECIFICATIONS OF ESP8266 D1 MINI	24
TABLE 3 PIN CONFIGURATION OF ESP8266 D1 MINI	24
TABLE 4 PIN CONFIGURATION AND FUNCTIONS OF TCA9548A MULTIPLEXER.....	26
TABLE 5 TECHNICAL SPECIFICATIONS IN THE PROGRAM	29
TABLE 6 ANGULAR DATA OF THREE SPINAL REGIONS (MEAN \pm SD).....	39
TABLE 7 ANGULAR DATA OF WRIST JOINT MOTION (MEAN \pm SD)	44

ABSTRACT

Data Acquisition system plays an important role in studying the biomechanics of joint motion, differentiate between pairs of movements done by a single joint, rehabilitation research, sports analysis and to provide the input orientation signal to the rehabilitation devices like exoskeletons etc. A real time portable motion sensing device is needed for the said purposes. Several conventional methods such as optical systems, magnetic systems, acoustic sensors etc. are used as motion sensing devices but there are certain drawbacks to these systems which prohibit using them in real time or to be used outdoors. To overcome the draw backs of the these methods, a real time portable motion sensing system was developed based on Inertial Measurement Unit (IMU). The IMU is a six-axis motion sensor with a 3-axis accelerometer and 3-axis gyro meter. The system developed gathers orientation data from different joints of the human body which serves as useful data to study the biomechanics of human joint motion and also serves to provide input signal to exoskeletons. This Data Acquisition system was utilized to carry out two studies; one on two different positions of human spine and the other on wrist joint motion.

CHAPTER 1

INTRODUCTION

Injuries of the spinal cord are different type of damages suffered by people that cause changes in the functionality of the spinal cord (1) (2). The changes in the functionality of the spinal cord result in reduction or complete loss of muscle function. It can also effect sensation in other parts of the body (3). These injuries in the cervical region (C4 to C7) result in mentioned losses in all four limbs (Tetraplegia) as well as in the torso of human body (1) (2).

The annual rate of spinal cord injuries is 15 to 40 incidents per million with causes ranging from injuries at workplace to road accidents and community violence to natural health deficiencies (bone/joint disorders and neuromuscular diseases) and accidents during leisure activities (4).

Spinal cord injuries affect the people around the patient; they can be immediate family as well as the society and community the patient lives in. Spinal cord injuries also play an intense role in harming the self-esteem of the patients as they need help with day to day activities which they could easily do before without any assistance. This has an impact on the mental health of patients with spinal cord injuries too.

1.1 EXOSKELETON

The role of robots for the purpose of rehabilitation is increasing rapidly. In order to cater for the lost functions of patients with spinal cord injuries, exoskeletons are designed. An exoskeleton is the outer/external skeleton that protects and supports human body in contrast to internal skeleton. They are rehabilitation structures that assist patients with their lost mobility. We are tackling with the patients who have tetraplegia, so the basic motion that those patients are deprived of is flexion and extension of torso. They are bed ridden and can only move their head/neck region.

Exoskeletons are not confined to just spinal cord injuries. It is a supportive structure which can be used for any other immobile structure in human body for example, Hand Exoskeleton.

Assisting patients having spinal cord injuries with sitting up and lying down does wonders for patients' self-esteem and health overall. It is reported that physiological improvements of human body activity result in less spasticity of muscles, improved bladder and bowel functions, decreased muscular pain, relief in pressure sores and higher energy levels (5).

1.2 DATA ACQUISITION

There are many areas of science and rehabilitation which directly benefit by conducting research and developing products to study biomechanics during human body movement. Such fields may include sports analysis, exoskeleton robots, interaction of human and machine etc.

Any exoskeleton essentially comprises of three parts: Mechanical Structure, data acquisition System and a control System. Data acquisition system has high importance in providing the input signal to the exoskeleton which is sent to the control system to then move the structure accordingly.

Data acquisition system is an essential part of the exoskeleton providing the input signal to the control system of exoskeleton. The DAQ system can also be utilized to study the biomechanics of human joints, differentiate between the pairs of movements done by a single joint, rehabilitation research and sports analysis etc.

1.3 DAQ TECHNIQUES

The usual techniques used to study Biomechanics of human body joints are:

- Optoelectronic systems
- Optical/camera based techniques
- Mechanical sensors
- Magnetic sensors
- Fiber optic sensors
- Acoustic motion capture systems

Optoelectronics systems are accurate when used with surface markers which are less in number. These systems, however, cannot work in outdoor spaces and does not give accurate information on orientation profile of spine.

Mechanical sensors are also accurate but they have the disadvantage of being inefficient and hard to use. Their range of motion is limited too.

Optical/camera based systems are considerably accurate and common in tracking human body motion. They also suffer from some disadvantages like following

- There isn't a clear line of sight between the subject and sensor

- Camera based systems are expensive
- They can only be used in an indoor or enclosed space
- They are prone to motion artifacts

Magnetic sensors tend to have negative reaction to metals and their own magnetic field gets distorted with other magnetic fields in the environment.

Fiber optic sensors measure the tilt or inclination based on the transmitted light's intensity. But one cannot measure orientation or rotation with fiber optic sensors because they are inflexible.

Acoustic motion capture systems also have a certain set of disadvantages which make them not ideal for upper body exoskeletons. For example, the emitter and receiver need to have a line of sight between them. They are also prone to disturbance and changes in temperature, humidity and wind.

1.4 OBJECTIVES OF THIS RESEARCH

A real time portable motion sensing device is needed to work as a data acquisition system and to study the biomechanics of human body joints. The conventional systems used which are discussed above cannot be used as a real time motion sensing device because of the drawbacks mentioned. Instead, a system with Inertial Motion Sensor (IMU) is recommended as replacement. With a wireless microcontroller unit, an inertial motion sensor can be developed into a real time portable motion sensing device and can be easily used while performing different tasks in a confined space as well as outdoors. An IMU caters to most problems associated with other methods for studying joint biomechanics.

An inertial measurement unit is a six-axes or nine-axes motion sensing device with built in accelerometer (3-axes), gyro meter (3-axis), magnetometer (3-axis) and sometimes comes with a temperature or pressure sensor as well (6). The main objectives of this research is to develop a real time, wireless data acquisition system based on an IMU to study the biomechanics of human joint, differentiate between pairs of movements on the basis of that data and to provide a DAQ system for a potential upper body exoskeleton system.

CHAPTER 2

LITERATURE REVIEW

Data acquisition systems have been discussed and developed over a considerable period of time. The early traces of such systems might not have involved the latest technology, hardware and software systems that are seen today. The techniques of how data is acquired from human body have also changed over time and vary with the application of research.

However with the passage of time data acquisition systems have also made considerable progress. Today, the exoskeletons have multiple degree of freedoms and DAQ systems are used for many other applications which requires for more robust systems and real time data to be taken and analyzed. Here we present the state of the art literature review in Data acquisition systems for various applications.

Wong et al (7) conducted a study in 2008 for trunk posture monitoring using inertial sensors. Sensor module consisted of one triple axes accelerometer, 3 one-axis gyroscopes and one DAQ & feedback system. Measurement from gyroscope & accelerometer could fluctuate. To eliminate this fluctuation error, an auto reset algorithm was implemented. Results of this research show that with the use of these 3-axes and 1-axis sensors, the changes in spinal curvature can be determined. Figure 1 shows subject with the spinal posture monitoring setup.

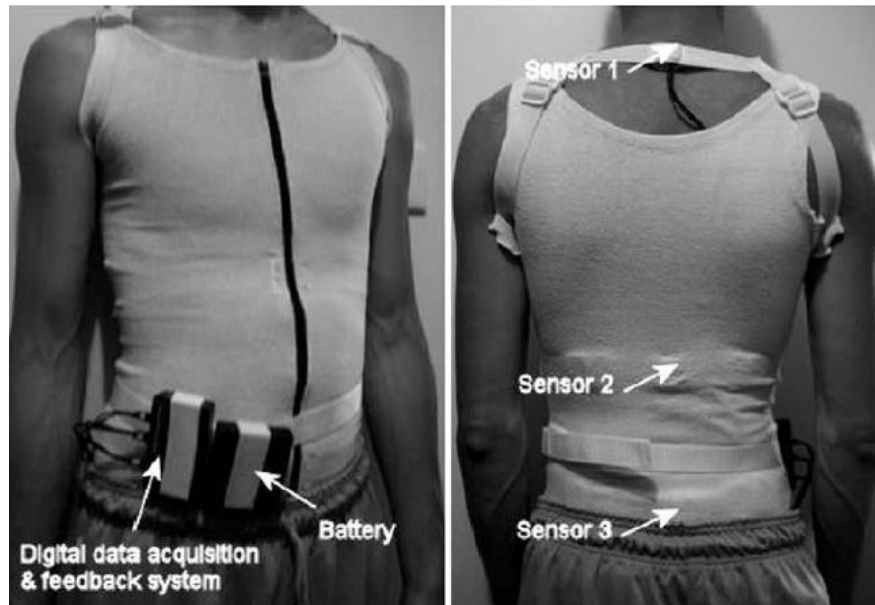


Figure 1 Subject with the Posture Monitoring System (7)

Ideal sitting posture was examined by measuring spinal curvature in four different sitting positions by Andrew P. Claus et al (8). A three dimensional electromagnetic tracking system with 5 sensors on spinous processes was used to acquire position data. Ultrasound images and manual method of palpitation was used to identify certain spinal landmarks. Accuracy of the measurements was affected by the presence of metallic objects.

In 2010, Jonathan M. Williams et al. (9) used a new measurement system to measure lumbar surface curvature.

The system consisted of a ribbon which was lined with fiber optic sensors. The research was concluded with the result that fiber optic system for motion analysis yields considerably good results for sagittal lumbar curvature. Figure 2 shows the attachment process of fiber optic and video system.

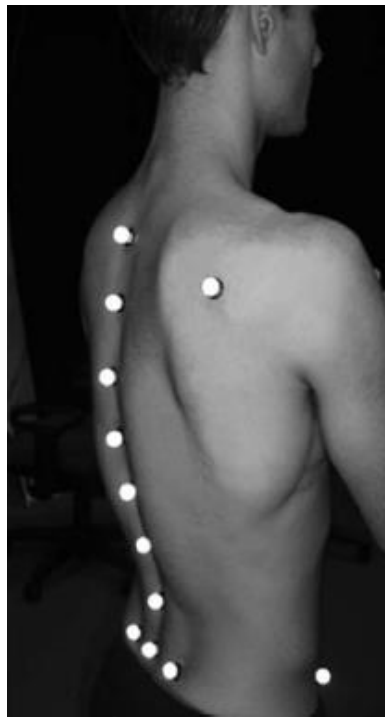


Figure 2 Fiber Optic and Video System Attachment (9)

A mobile sensing and real time spine health monitoring system was developed by Noura Farra et al. in 2011 (10). The sensing system used had inclinometers and load cells as sensors. Image acquisition method used was Photogrammetric X-Ray. Structural information is gathered using the system and spinal health is monitored. The imaging system was able to find the Cobb angle in an automated, non-invasive and simple fashion. Figure 3 shows the spine stress monitoring system worn by the patient.



Figure 3 Spine Stress Monitoring System worn by patient (10)

Daniel Baumgartner et al. (11) used a magnetic resonance imaging (MRI) scanner to measure the changes in the angles of the spinal cord along the sagittal plane for sitting positions. The three positions being, forward inclined, reclined and upright. The chair that was used was MRI compatible and adapted to be used in the scanner. Figure 4 shows the MRI compatible chair to study sitting posture in different positions.



Figure 4 MRI Compatible chair to study posture during different sitting positions (11)

Aaron Gipsman et al. (12) used surface topography paired with reflective markers and 4-D Formetric camera (13) for static imaging of the spine. This system is used to analyze surface asymmetry and to identify bony landmarks. One prominent advantage of surface topography is that it avoids exposure to radiation. The downside of this study is the overall cost spent on the

whole setup. Laboratory equipment required for analyzing the dynamic changes in spinal curvature and position is expensive. The results of this study show that this technique provides reliable measurements for healthy subjects with same day repeat measurements. The error ranges were comparable to the current gold standard in dynamic motion analysis. Figure 5 shows the Formetric 4D device used in the study.



Figure 5 Formetric 4D Device (12)

Lei Yan et al. (14) designed a lower limb exoskeleton robot and a DAQ (Data Acquisition system) system plus a control system is developed to assist the patient's walking abilities under special circumstances.

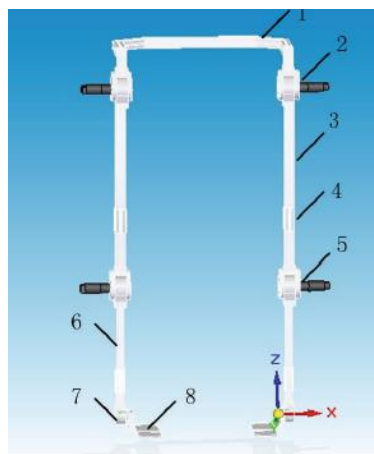


Figure 6 The Mechanical Structure Diagram of Robotic Exoskeleton (14)

Figure 6 shows the mechanical structure design of the exoskeleton. Effective information about the desired movement of the body is collected through the DAQ system in real time and fed to the control system to move the structure according to the information received. The DAQ system consists of four types of sensors including acceleration sensors, gravity sensors, pressure sensors, and gyroscopes. Digital accelerometer is used to measure static acceleration of gravity as well as dynamic acceleration. Processing is done with the ZigBee wireless transmission module. The sensors help collect location and movement information.

Primoz Poredos et al. (15) worked on camera based method to determine the human spine curvature. Measurements were taken from the thoracic and lumbar spine with three dimensional triangulation techniques. Measurements from the back, however, were taken with a three dimensional profilometer. The process becomes accurate, quick and non-invasive with these methods. The proposed technique in this research could replace the normally used methods because it ensures safety of the patient while measuring the spinal curvature. Figure 7 shows the triangulation measurement scheme used in this research.

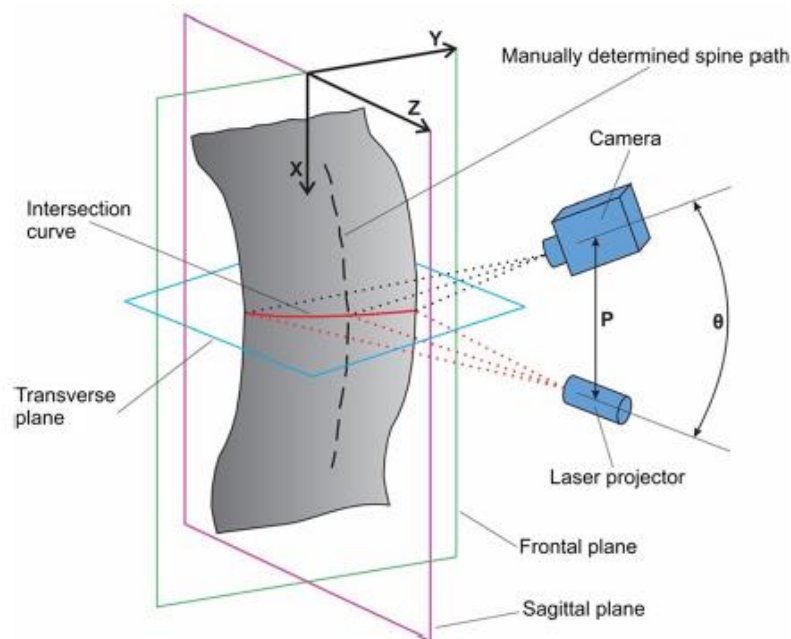


Figure 7 The Triangulation Measurement Scheme (15)

Stefan Schmid et al. (16) conducted a study using motion capture system based on skin markers for measurement of spinal curvature. The results of this study inferred that skin marker-based motion capture techniques can be used for the non-invasive assessment of spinal curvature angles in the sagittal and frontal planes. Therefore skin markers should be used for measurement of movement and postural change during dynamic activities like walking and not for measuring absolute angles.

Nabilla S. M. Kamil et al. (17) studied the postural angle change when doing back muscle tasks by making the ageing female workers do certain computer tasks. The subjects selected were seventeen in number, greater than or 50 years of age. Postural angles of the back were measured from the pelvis area and the upper trunk area. Inline 2 dimensional inclinometers (18) were attached with the help of a tape on bony areas at the T2 section and sacrum. Measurements were recorded in the sagittal plane. Results of the study showed that posture of the upper trunk gets affected by activities of back muscles and that a neutral posture of back reduces the activities of muscles in aging women who perform computer tasks.

Björn Krystek for his research developed a wearable electronic sensor array and a measuring unit for spine and postural analysis (19). A prototype was built using gyroscopic sensors (with integrated accelerometers) and the Arduino (20) platform along with a software to interpret the measurements as visual assistance. In general, the approach using gyroscopic or inertial measurement to monitor spinal posture proved to be a good option when a small device is needed. By using MEMS components, inertial measurement units provide the best options for hiding the sensors. Figure 8 shows the sensors attached to the patient.

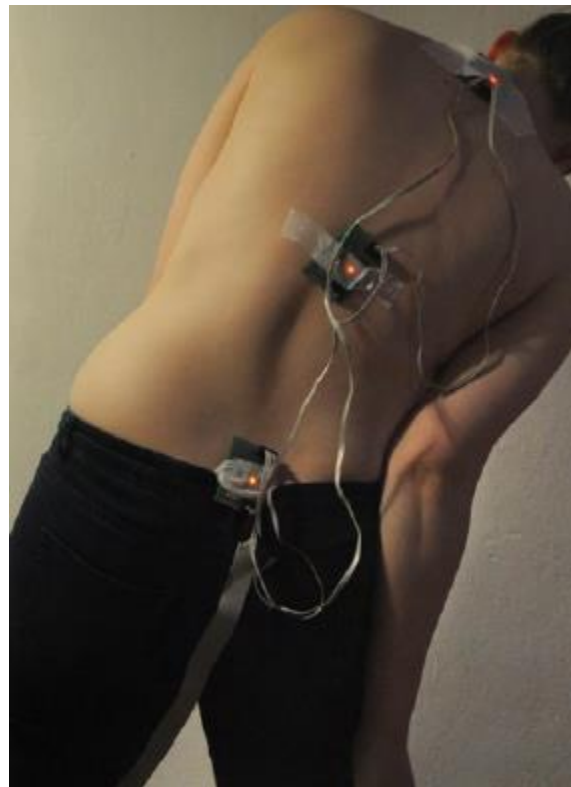


Figure 8 Sensor setup attached to the patient (19)

In the work done by Gheorghe Daniel Voinea et al. (21) a wearable system was used for measurement and modeling of spine cord. The study was performed for the purpose of medical rehabilitation.

The spine monitoring system developed was made out of inertial sensors which measured and reconstructed the spine's posture. The simulations obtained in the study showed good results with a mathematical model that could reconstruct the human spine. Figure 9 shows the spine monitoring system with flexible wearable straps.



Figure 9 Wearable spine monitoring system with flexible straps (21)

Andualem T. Maereg et al. (22) developed an Opto-Inertial six degrees of freedom hand for pose-tracking system. The tracking part of the hand is optical with a Playstation eye camera and two Infra-red LEDs while the inertial portion has an IMU module which is made up of a three-axes gyroscope, a three-axes accelerometer and a three-axes magnetometer on a single IC.

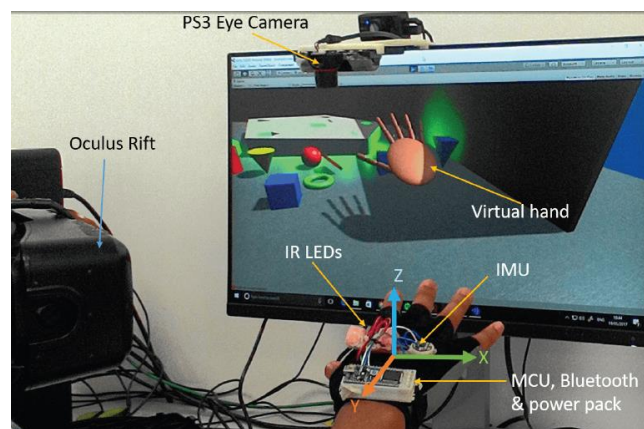


Figure 10 Virtual Reality 6 Degrees of Freedom Experimental Setup (22)

This study concluded with the result that due to complimentary pros and cons, the combination of inertial and optical systems for pose tracking in six degrees of freedom produced better results than when these systems are used separately. Figure 10 shows the virtual reality six degrees of freedom experimental setup.

CHAPTER 3

METHODOLOGY

Inertial sensors are sensors based on the principle of inertia. These sensors range from MEMS (microelectromechanical) sensors which measure a few squares in mm up to gyroscopes that are accurate and measure up to 50 cm in diameter.

An inertial measurement unit (IMU) is an electronic device that consists of an accelerometer, gyrometer and magnetometer or sometimes combination of all three to measure the distance travelled angular change due to a body's rotation and effect of magnetic field on both these measurements. Accelerometers are used to detect linear acceleration and rotational rate using the gyroscopes. Magnetometers are used as a heading reference.

An inertial navigation system (INS) does not depend on external measurements; it uses the built in gyroscope, accelerometer and magnetometer to measure the position of an object precisely. Therefore an INS can be taken to any remote area where other navigation systems are not available.

3.1 YAW PITCH ROLL

Human body joint rotations in three dimensions can be described in the form of aviation terminologies, also known as Euler angles as Yaw, Pitch and Roll. In simple words, yaw is the rotation of the body around x-axis, pitch is the rotation of the body around y-axis and roll is the rotation of the body around z-axis. The combination of these three rotations can be used to represent any arbitrary rotation. These rotations can also be referred to as rotation about the current original axis to form a new frame. Figure 11 explains the change of frames concept.

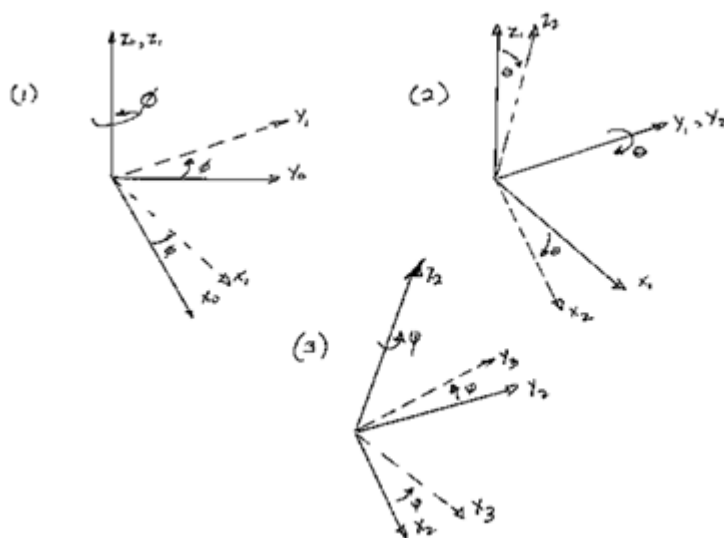


Figure 11 Rotations in Frames: Euler Angles

The yaw axis is perpendicular to the object with its origin pointed toward the bottom of it and at its center of gravity. Yaw motion of the object is movement of the object's front from side to side. The pitch axis is at right angle to the yaw axis and parallel to the object's sides. A pitch motion is an up or down movement of the front of the object.

The roll axis is at right angles to the other two axes, pointed towards the front end of the object and its origin at the center of gravity. The rolling motion of an object is the up down movement of the left and right sides of the object.

3.2 SPINAL CURVES

The shape of an adult human's spine is an S-Curve. The neck and lower back region has a concave curve, and the thoracic and sacral region has a convex curve (Figure 12). These curves act as a shock absorber, increase range of motion and maintain body's balance.

A healthy spine is the result of strong bones and muscles, sensitive nervous system and tendons and ligaments with high flexibility. The weakening of these factors mean an unhealthy spine as a result which might result in the following abnormalities:

- Lordosis is the abnormal lumbar spine curve.
- Kyphosis is the abnormal thoracic spine curve.
- Scoliosis is the side to side abnormal curve.

Good posture is obtained by maintaining the body's natural balance and to stand, sit, walk and lie in such a manner that least strain is put on the spinal cord.

3.2.1 VERTEBRAE

The spinal column is made up of 33 bones fused together that are called Vertebrae. These vertebrae are divided into regions and then numbered and named according to the region they belong to (Figure 12). The coccyx and sacrum vertebrae are fixed while the upper 24 are moveable.

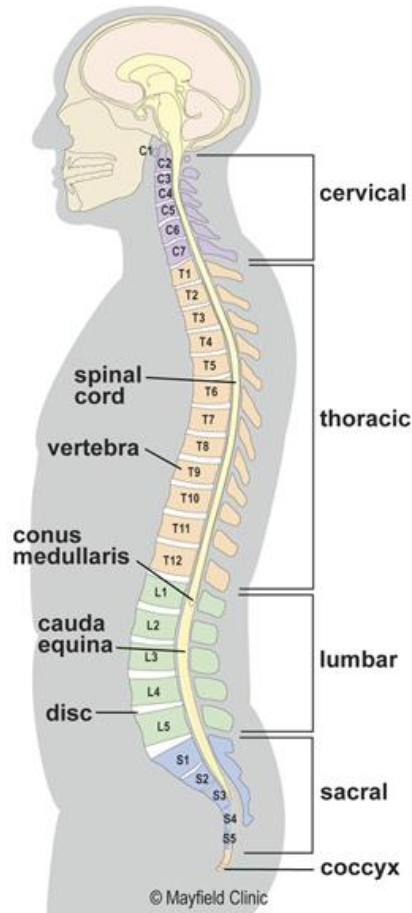


Figure 12 Spinal Curves

3.2.2 CERVICAL, THORACIC AND LUMBAR SPINE

Each region's vertebrae have features that make them unique and help them perform different tasks.

Cervical (neck) region– the vital function of this region is to provide support for the head. There are seven vertebrae in the cervical region numbered from C1 to C7. The neck region connects to the skull and it has two specialized vertebrae so it has the highest range of motion in the human body. C1 and C2 vertebrae are in the neck region. C1 has the shape of the ring and is used for the yes motion while C2 has the shape of a peg that is used for the No motion of the head.

Thoracic (mid-section of back) region- the vital function of thoracic region is to protect the lungs and heart and hold rib cage that holds the heart in place. Thoracic region has twelve vertebrae numbered from T1 to T12. However, the range of motion of thoracic spine, unlike the cervical region, is limited.

Lumbar (lower section of back) region- the vital function of the lumbar spine is to hold the weight of the body. There are five vertebrae in the lumbar spine numbered from L1 to L5. The vertebrae in this area are larger because they carry the stress and weight of lifting very heavy objects hence more problems and injuries are those of lumbar spine.

3.3 INERTIAL NAVIGATION SYSTEM

INS (Inertial Navigation System) is a six-axes or nine-axes motion sensing device with built in accelerometer (3-axes), gyro meter (3-axis), magnetometer (3-axis) and sometimes comes with a temperature or pressure sensor as well (6) (23).

3.3.1 ACCELEROMETER OF THE IMU

The accelerometer's measurement relies on gravitational pull which is that of 9.8 m/s^2 equal to 1 g. In an ideal situation, there are no external forces acting on the accelerometer and acceleration's magnitude is 1 g. In that case, the acceleration vector's position gives us the sensor's rotation information. In a special case where z-axis is parallel to the gravitational acceleration vector, the computation of rotation around z-axis becomes impossible.

Analog accelerometers give a voltage level as an output while digital ones give information via serial protocols such as SPI and I2C. Figure 13 shows the inertial measurement unit with Yaw, Pitch, Roll (X, Y, and Z) axes directions.

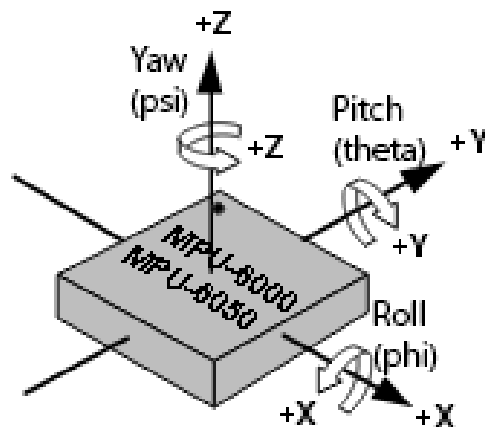


Figure 13 Inertial Measurement Unit

An accelerometer has a zero gravity voltage level which can be found in the specifications and is common in all of them. Accelerometers' sensitivity is represented in mV/g . The final value is determined by dividing the zero gravity voltage level by accelerometer's sensitivity.

3.3.2 GYROMETER OF THE IMU

A gyroscope gives information about the rate of change of rotation, not the orientation itself. The gyrometer's position must be initialized first, this can be done with the help of accelerometer. Then angular velocity (ω) is measured around each of the three axes at measured time intervals (Δt).

$$\omega \times \Delta t = \text{change in angle}$$

The orientation angle obtained will be the original angle plus the change that has occurred. The increments of $\omega \times \Delta t$ result in small amount of errors which during integration start adding up and are difficult to remove.

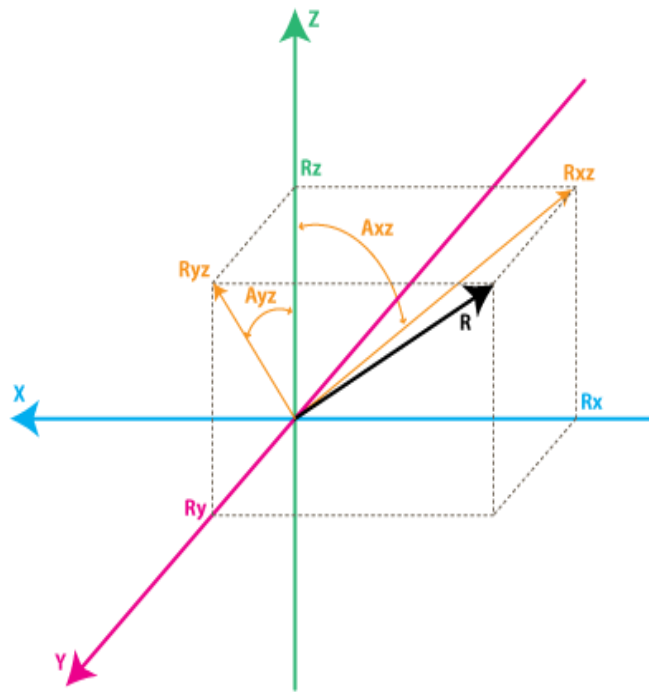


Figure 14 Angles from a Gyroscope

As shown in Figure 14, individual gyroscope measures the rotation around an individual axis:

A_{xz} – is the orientation angle measured between the R_{xz} (projection of R) and Z axis

A_{yz} – is the orientation angle measured between the R_{yz} (projection of R) and Z axis

The time rate of change of these orientation angles is what the gyroscope measures.

3.4 INITIAL PATHWAY TAKEN FOR PROJECT

(IMU DISTANCE APPROACH)

Initially the pathway of the project was to find accurate real time positioning with the IMU. For that purpose, the accelerometer of IMU was utilized to calculate the real time distance travelled by the IMU or by the object to which it was attached. Raw data was taken from motion sensor and analyzed.

These raw values were converted into acceleration values by applying double integration method. With the help of first integration, velocity was found for each converted value of acceleration. The second integration converts the velocity into distance. Formulas are shown below.

First time Integration: Converting acceleration into Velocity

$$v(t) = v(t_0) + \int_{t_0}^t a(u)du.$$

Second time Integration: Converting velocity into Distance

$$s(t) = s(t_0) + \int_{t_0}^t v(u)du.$$

3.5 EXPERIEMENTS PERFORMED WITH ACCELEROMETER

In one of the many experiments that were performed with using the accelerometer of the IMU, the sensor was moved along 10 cm which equals 0.1 m. The graph showing raw acceleration values collected from the IMU is shown in Figure 15 at the top.

A differential filter was then applied on the Raw values to correct the DC shift (baseline shift). The third graph shows the result of first integration on the filtered signal. This gives us velocity and another integral is applied on the velocity to get distance as shown in part four of Figure 15.

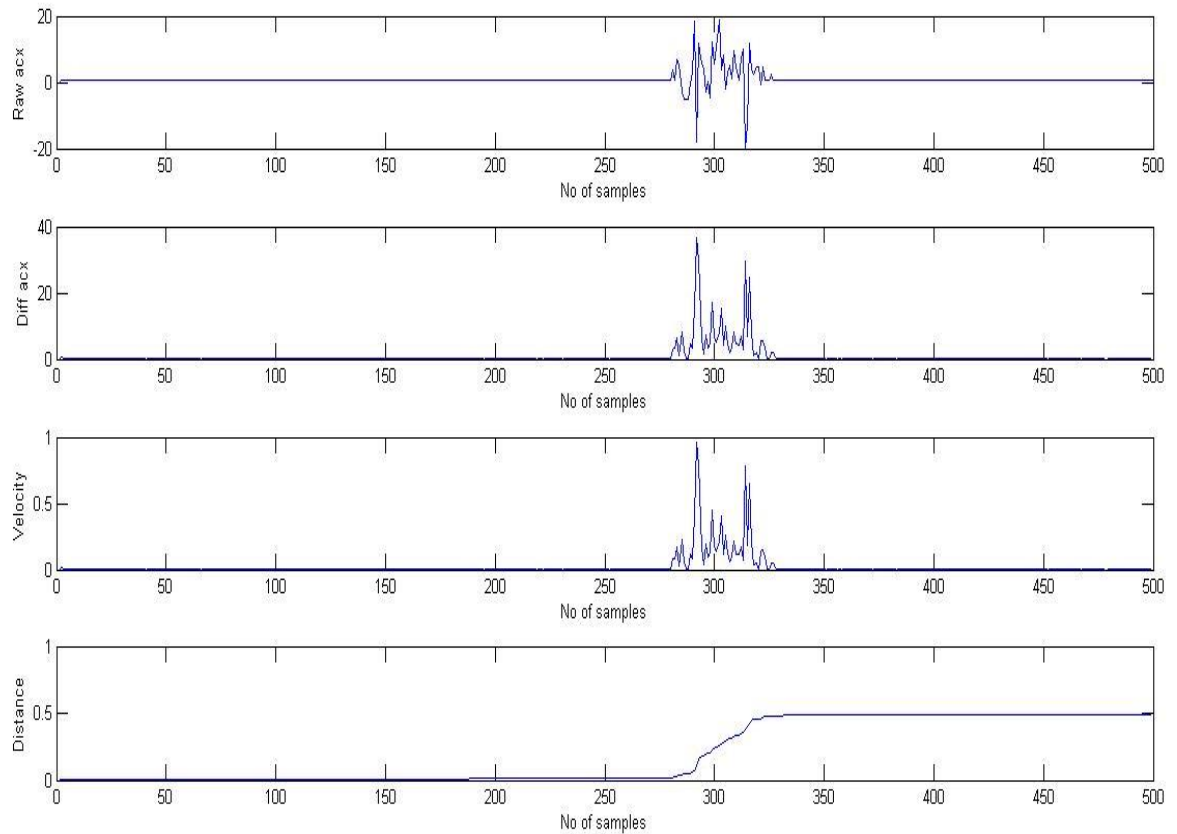


Figure 15 Finding Distance using Accelerometer of the IMU

Between the samples 270 to 350, the sensor was moved along the said distance of 0.1 m (1 cm). After calculations and double integration above, the calculated mean value of distance for this experiment was 0.277

The mean value was greater than our desired value of 0.1 m. Some of the experiments yielded better results than this one but the mean value always more or less than the desired value. With double integration, error accumulates over time which for larger distances becomes inevitable to remove. Hence, the pathway of the project was changed to using the gyrometer of the IMU instead of the accelerometer.

3.6 GYROMETER BASED APPROACH

The gyrometer of the IMU gives values in radians which are then converted to degrees. The gyro gives readings from +90 to -90 in each direction it is moved. Yaw pitch roll in x, y and z directions all ranging from +90 to -90 depending upon the orientation of the sensor.

It takes about 8 seconds of no motion after startup for an un-calibrated sensor to produce steady values with the DMP. Once this initial calibration occurs, the roll, pitch, and yaw values should be very stable, especially the roll and pitch.

The yaw value is subject to a very tiny amount of drift since there is no magnetometer present in the device, and no absolute reference point available for the heading (yaw). Roll and pitch are calculated from the gyro movements as well, but fused with gravity data from the accelerometer and they are stable enough once calibration is done.

It is common for the pitch/roll values to be non-zero even after calibration, since it means the sensor isn't 100% exactly "level" with respect to gravity.

This is hard to measure precisely with a carpenter's level or something because the MPU chip itself is so small, but one should be able to fix the values by slightly changing the X/Y tilt of the device.

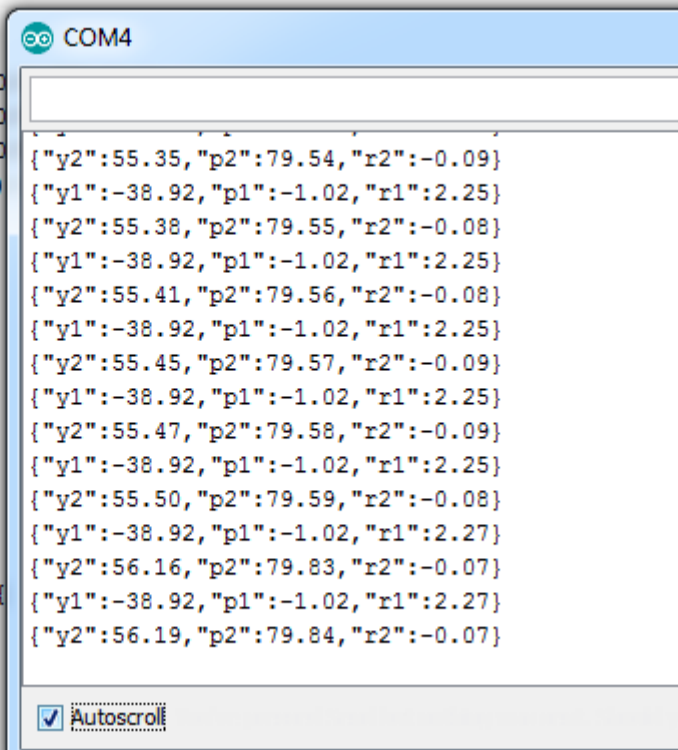
For sample values, the yaw pitch roll for two sensors is shown in Figure 16

```
+ "{";
codeValue("y1", ypr1[0]*180
codeValue("p1", ypr1[1]*180
codeValue("r1", ypr1[2]*180
/Vals); Serial.print("\n")

ze activity
ze;
linkState);

*****//////////

ifoCount2 < packetSize2) {
i get INT_STATUS byte
```

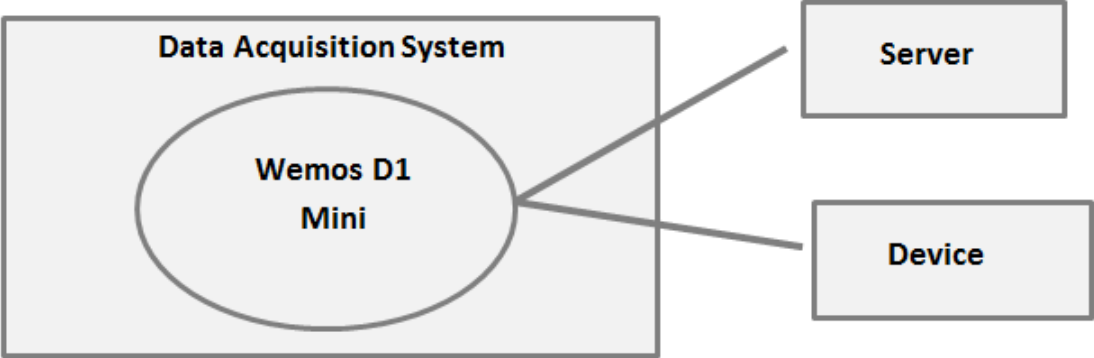


```
{"y2":55.35,"p2":79.54,"r2":-0.09}
{"y1":-38.92,"p1":-1.02,"r1":2.25}
{"y2":55.38,"p2":79.55,"r2":-0.08}
{"y1":-38.92,"p1":-1.02,"r1":2.25}
{"y2":55.41,"p2":79.56,"r2":-0.08}
{"y1":-38.92,"p1":-1.02,"r1":2.25}
{"y2":55.45,"p2":79.57,"r2":-0.09}
{"y1":-38.92,"p1":-1.02,"r1":2.25}
{"y2":55.47,"p2":79.58,"r2":-0.09}
{"y1":-38.92,"p1":-1.02,"r1":2.25}
{"y2":55.50,"p2":79.59,"r2":-0.08}
{"y1":-38.92,"p1":-1.02,"r1":2.27}
{"y2":56.16,"p2":79.83,"r2":-0.07}
{"y1":-38.92,"p1":-1.02,"r1":2.27}
{"y2":56.19,"p2":79.84,"r2":-0.07}
```

Figure 16 Yaw, Pitch, Roll values from Gyrometer of the IMU

3.7 PORTBALE DEVICE

Wi-fi based MCU is being used in the DAQ system, which means that each IMU sensor module paired with the wi-fi module can be used as individual portable motion sensing device which is the ultimate goal in this research.



CHAPTER 4

SYSTEM DEVELOPMENT

The main hardware components used in this research were three in number. Inertial Measurement Unit MPU6050 was used as a motion sensor. Because data had to be taken from multiple joints on human spine and hand, therefore more than one sensor was used to record the orientation data. For that purpose, an I2C based multiplexer TCA9548A was used. The microcontroller unit used was Wi-Fi enabled MCU, Wemos D1 Mini ESP8266. It transmits the data wirelessly over Wi-Fi so it can be accessed and observed anywhere.

4.1 INERTIAL MEASUREMENT UNIT (MPU6050)

The inertial measurement unit used in this research is MPU6050 which consists of a 3-axes gyrometer, a 3-axes accelerometer and a temperature sensor.

The MPU-6050 is an integrated 6 axes device for tracking motion. It is a combination of three axes gyrometer , a three axes accelerometer , a temperature sensor and an on board Digital motion processor (DMP). The serial protocol that it uses is I2C. With an external magnetometer and I2C bus, the MPU 6050 provides a 9 axes motion fusion output.

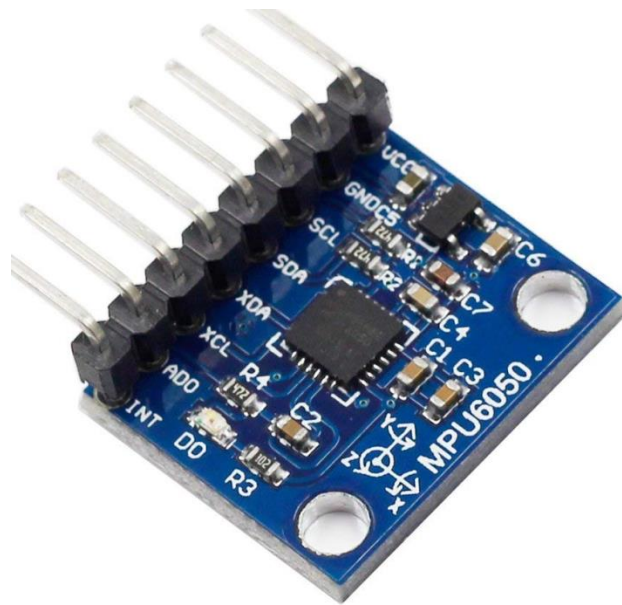


Figure 17 MPU6050 Motion Sensor (24)

4.1.1 DIGITAL MOTION PROCESSOR

The digital motion processor in MPU6050 runs six axes motion fusion algorithms to provide information about the object's position and orientation. The sensor can be connected with an

external sensor like a magnetometer or an auxiliary I2C and without the involvement of the system's processor; a full set of data from sensors is collected.



Figure 18 MPU 6000 Family Block Diagram

4.1.2 PIN CONNECTIONS OF MPU6050 WITH ESP8266

Table 1 shows the pin connections of motion sensor MPU6050 with the ESP8266 D1 mini followed by the wiring diagram in Figure 19.

Table 1 Pin Connections of MPU6050 with ESP8266

MPU6050	ESP8266 Wemos D1 Mini
Vcc	3.3V
GND	GND (0V)
SCL	D1 (GPIO5)
SDA	D2 (GPIO4)
AD0	GND (At I2C Address 0x68) 3.3V (At I2C Address 0x69)
INT	D8 (GPIO15)

*GPIO: General Purpose Input Output

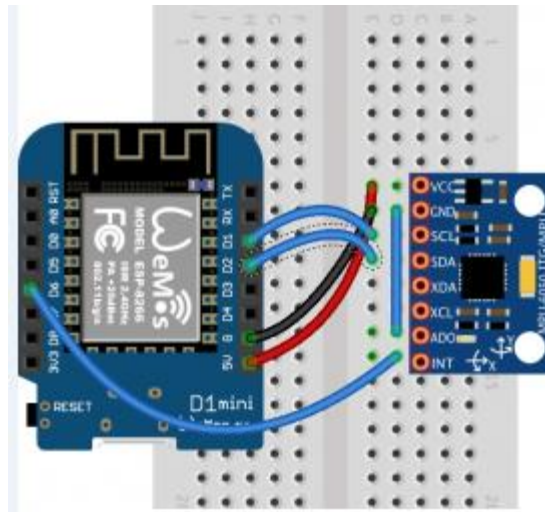


Figure 19 Wiring diagram of MPU6050 with Wemos D1 Mini

Figure 19 shows the key blocks and functions of the MPU60X0 family.

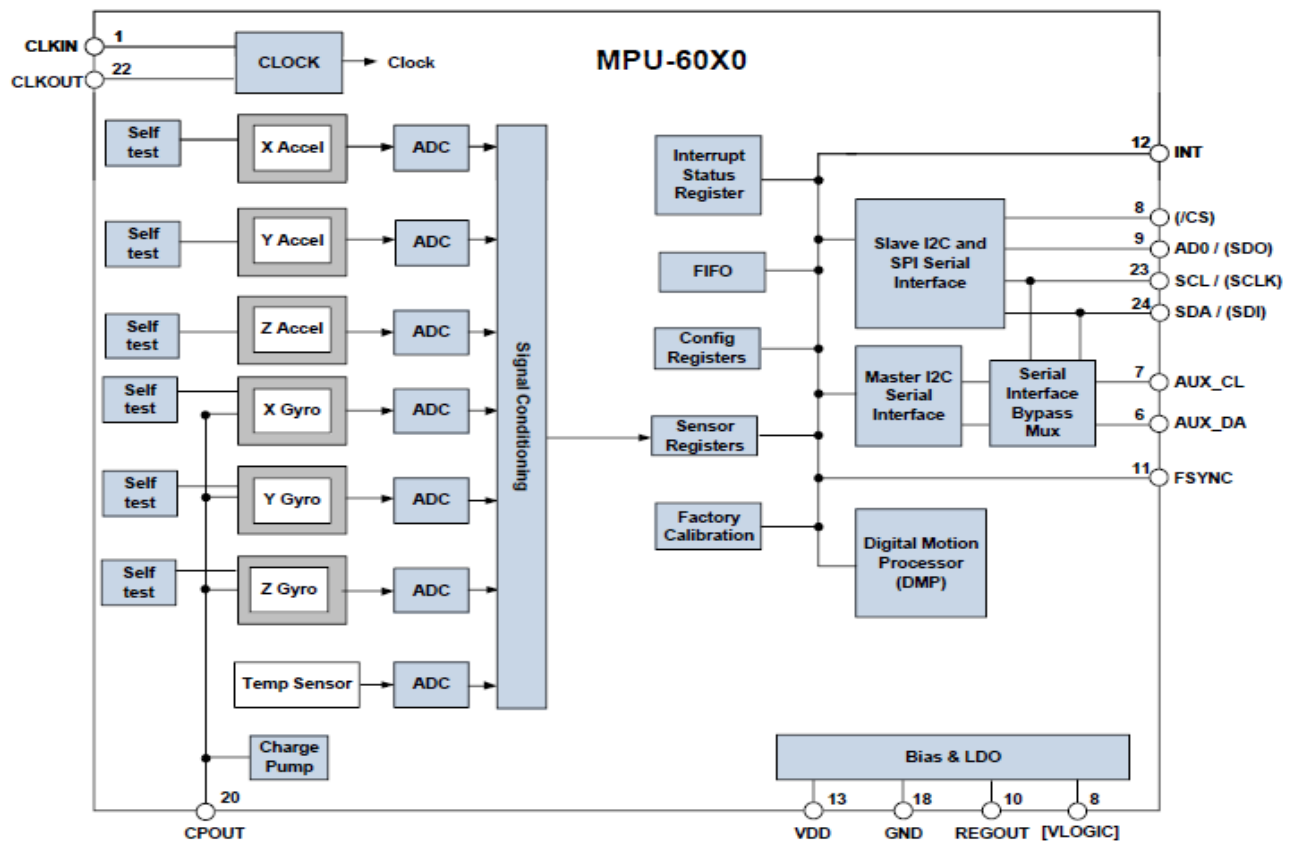


Figure 20 Block Diagram of the MPU60X0 Family

4.2 ESP-8266 Wi-Fi Based MCU

Wemos D1 mini is like a "little Arduino with wifi" . It's based around the ESP8266, has one analogue port and 11 digital ports. It's programmed via micro-USB (or remote flash via wifi). It can be used with the Arduino IDE, micropython or NodeMCU. It runs from 5V or 3.3V. Logic levels are 3.3V for all ports.

Using the ESP8266 with MPU6050 makes it possible for each sensor to act as a node and transmit the values it gathers over Wi-Fi. This way, the data acquisition system is not confined to a space and can be remotely used anywhere. Table 2 and Table 3 list the technical specifications and pin configuration of the board respectively.

Table 2 Technical Specifications of ESP8266 D1 Mini

Specs	Detail
Operating Voltage	3.3 V
Digital I/O Pins	11
Analog Input Pins	1 (Max Input: 3.2 V)
Clock Speed	80 MHz/160 MHz
Flash	4M bytes
Length	34.2 mm
Width	25.6 mm
Weight	3g

Table 3 Pin Configuration of ESP8266 D1 Mini

Pin	Function	ESP8266 Pin
TX	TXD	TXD
RX	RXD	RXD
A0	Analog Input, Max 3.3V Input	A0
D0	IO	GPIO16
D1	IO, SCL	5
D2	IO, SDA	4
D3	IO, 10k Pull-up	0
D4	IO, 10k Pull up, BUILTIN_LED	2
D5	IO, SCK	14
D6	IO, MISO	12
D7	IO, MOSI	13
D8	IO, 10k, Pull-down, SS	15

G	Ground	GND
5V	5V	-
3V3	3.3V	3.3V
RST	RESET	RST

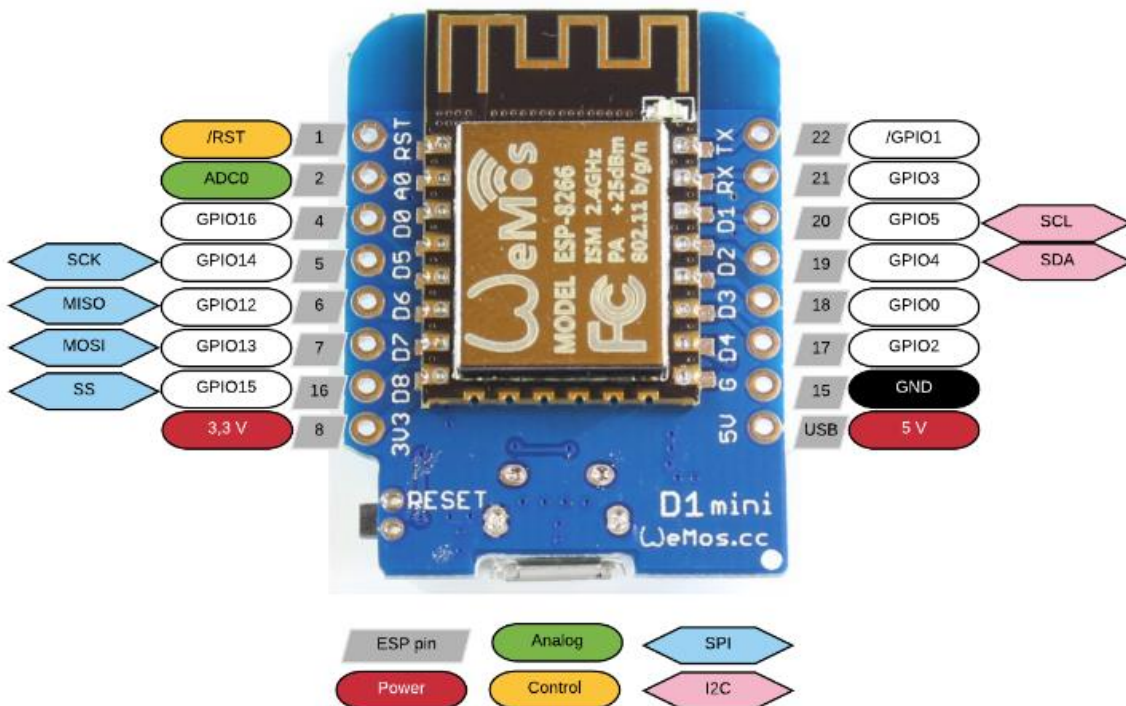


Figure 20 ESP8266 Wemos D1 Mini

4.3 TCA9548A I2C Multiplexer

TCA9548A is an I2C based multiplexer. This multiplexer has 8 bidirectional switches that are controlled by the I2C bus. There are two main pins for the data and clock lines: SCL and SDA. These are attached to the microcontroller's SCL and SDA pins.

The rest of the data and clock lines are total eight in number which are connected to the number of sensors from which data needs to be taken. Each of the channel to which the sensors are attached can be controlled and made On/Off with the help of programming.

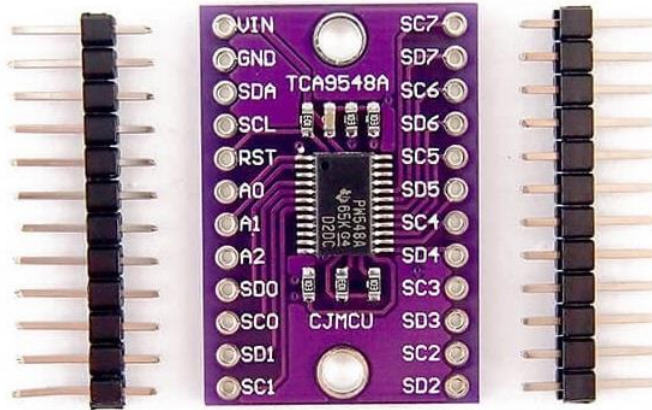


Figure 21 TCA9548A Multiplexer

Table 4 Pin Configuration and Functions of TCA9548A Multiplexer

Pin	Type	Description
A0	INPUT	Address Input 0. Connect directly to Vcc or Ground
A1	INPUT	Address Input 1. Connect directly to Vcc or Ground
RESET	INPUT	Active-low reset input. Connect to VCC or VDPUM through a pull-up resistor, if not used.
SD0	I/O	Serial data 0. Connect to VDPU0 through a pull-up resistor.
SC0	I/O	Serial clock 0. Connect to VDPU0 through a pull-up resistor.
SD1	I/O	Serial data 1. Connect to VDPU0 through a pull-up resistor.
SC1	I/O	Serial clock 1. Connect to VDPU0 through a pull-up resistor.
SD2	I/O	Serial data 2. Connect to VDPU0 through a pull-up resistor.
SC2	I/O	Serial clock 2. Connect to VDPU0 through a pull-up resistor.
SD3	I/O	Serial data 3. Connect to VDPU0 through a pull-up resistor.
SC3	I/O	Serial clock 3. Connect to VDPU0 through a pull-up resistor.
GND	Ground	Ground
SD4	I/O	Serial data 4. Connect to VDPU0 through a pull-up resistor.
SC4	I/O	Serial clock 4. Connect to VDPU0 through a pull-up resistor.
SD5	I/O	Serial data 5. Connect to VDPU0 through a pull-up resistor.
SC5	I/O	Serial clock 5. Connect to VDPU0 through a pull-up resistor.
SD6	I/O	Serial data 6. Connect to VDPU0 through a pull-up resistor.
SC6	I/O	Serial clock 6. Connect to VDPU0 through a pull-up resistor.
SD7	I/O	Serial data 7. Connect to VDPU0 through a pull-up resistor.
SC7	I/O	Serial clock 7. Connect to VDPU0 through a pull-up resistor.
A2	INPUT	Address Input 2. Connect directly to Vcc or Ground
SCL	I/O	Serial clock bus. Connect to VDPUM through a pull-up resistor.
SDA	I/O	Serial data bus. Connect to VDPUM through a pull-up resistor.
VCC	POWER	Supply Voltage

VDPUX is the pull-up reference voltage for the associated data line. VDPUM is the master I2C reference voltage and VDPU0-VDPU7 are the slave channel reference voltages.

Figure 22 shows the application diagram of TCA9548A multiplexer.

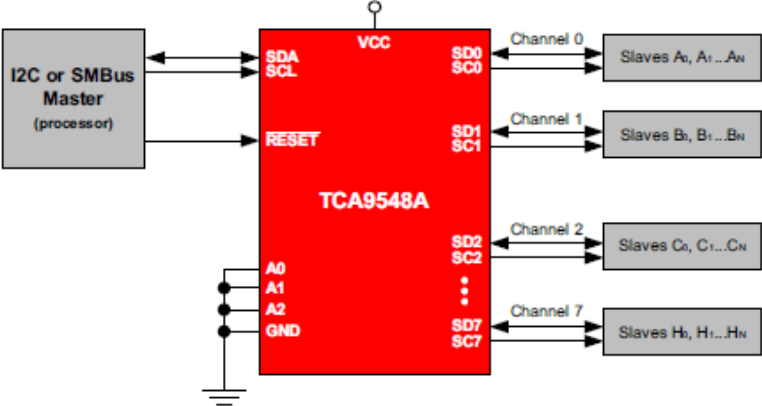
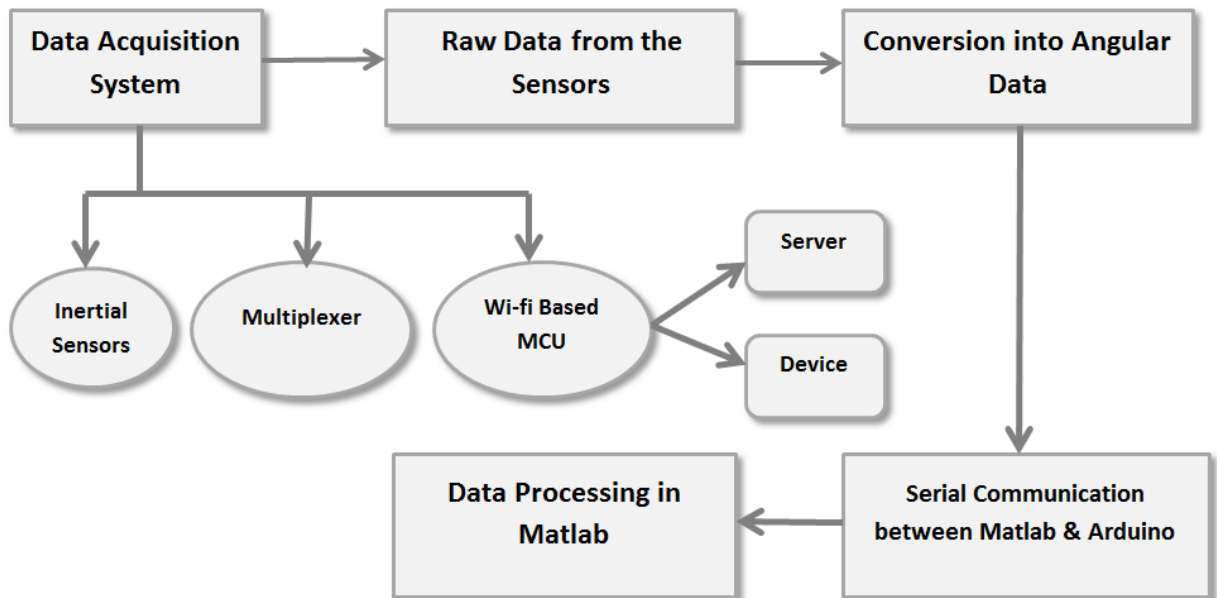


Figure 22 Application Diagram of TCA9548A multiplexer

CHAPTER 5

EXPERIMENTATION AND RESULTS

The flow of the project is shown in the block diagram below. The data acquisition system developed is used to get data from sensors. Sensors give raw data which then is converted into understandable orientation data within the program. The useful data obtained from the sensors is then sent over serially to MATLAB for further analysis. The data is tuned and processed in MATLAB to get further results. It is important to note that the data acquisition system consists of inertial sensors, a multiplexer and a Wi-Fi based microcontroller unit that communicates with both the server and the device. The use of *wi-fi based controller* also means that the system is not confined to an indoor space. It can be used remotely to take real time data. Hence each sensor acted as a portable device on its own.



5.1 CALIBRATION

The first step was to calibrate the accelerometer and gyrometer of each of the sensors separately. The calibration is done with the method of tilting the sensor at right angles in each of the three axes and recording the offset of the values. Next the offset is subtracted or added in order to get the gyrometer's value to 90 degrees. Similarly, when doing the calibration of accelerometer, the value on all three axes should be +/-16384 or 32767 on each axis for a sensitivity of +/- 2g. The sensitivity for gyrometer and accelerometer is +/- 2000 %/s and +/- 16g respectively.

Table 5 Technical Specifications in the Program

Specs	Detail
DLPF	State: ON
Sample Rate	200Hz
Gyrometer Output Rate	1 KHz
FIFO Rate	100Hz
DMP Output Frequency	50 Hz

*DLPF: Digital Low Pass Filter

5.2 APPLICATIONS OF THE DAQ SYSTEM

The data acquisition system developed was tested for two applications. One was to study the orientation of human spine. The cervical, lumbar and thoracic angles were recorded for sitting and lying down positions of a human body. The other study was performed on the wrist joint to differentiate between different pairs of hand movements.

5.2.1 BIOMECHANICS OF THE SPINE

To get the positioning data from human spine, three IMUs were attached to the spine of subject. One sensor was attached to the cervical area, one to the thoracic area and one to the lumbar region. Rotations around the x-axes for separate sensors were analyzed along the sagittal plane. Readings were taken from 5 subjects in following two positions:

- Sitting
- Lying down

The setup for experiment on spine is shown in Figure 23.

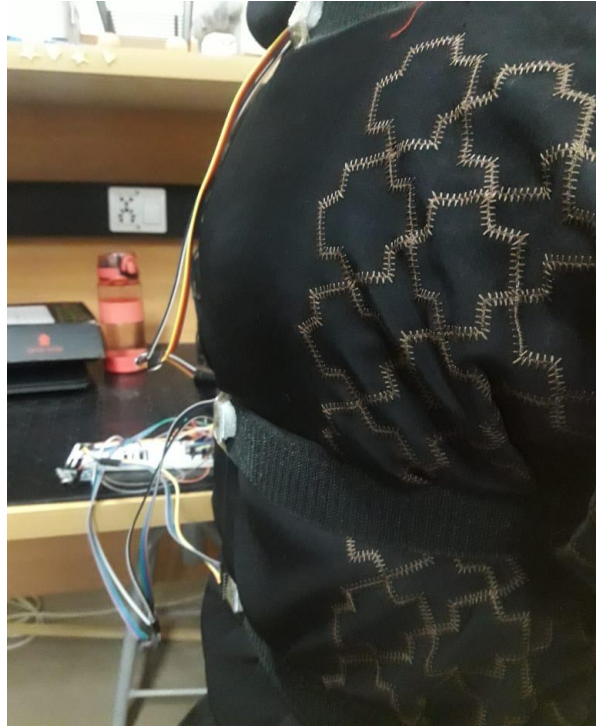


Figure 23 Setup for the Experiment on Spine

The IMU gives rotational data around its three axes. But in this case when sitting and lying down positions are taken into account, the movement occurs along the x-axis of the sensor. This plane is the sagittal plane. Along the sagittal plane of human body, flexion and extension movement of the spine is happening.

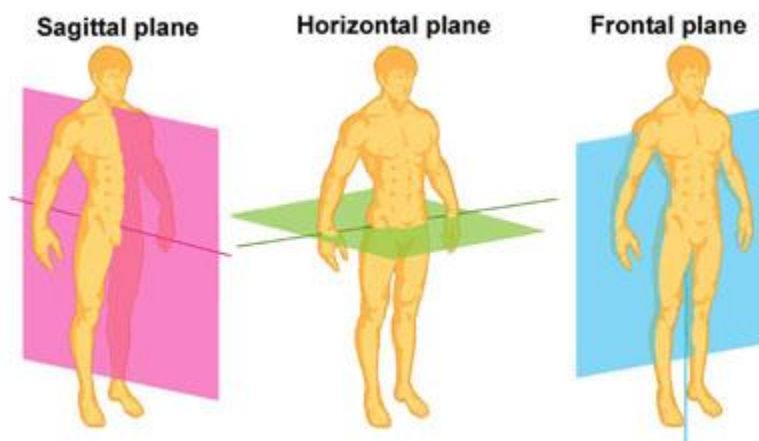


Figure 24 Planes of human body rotations

Hence, it is the sagittal plane that is important to analyze when sitting and lying down and going from first position to the second or vice versa. The orientation of the sensors placed on subjects

is as such that the orientation data from flexion/extension is obtained from the x axis of the sensor. This is shown in Figure 25 below.

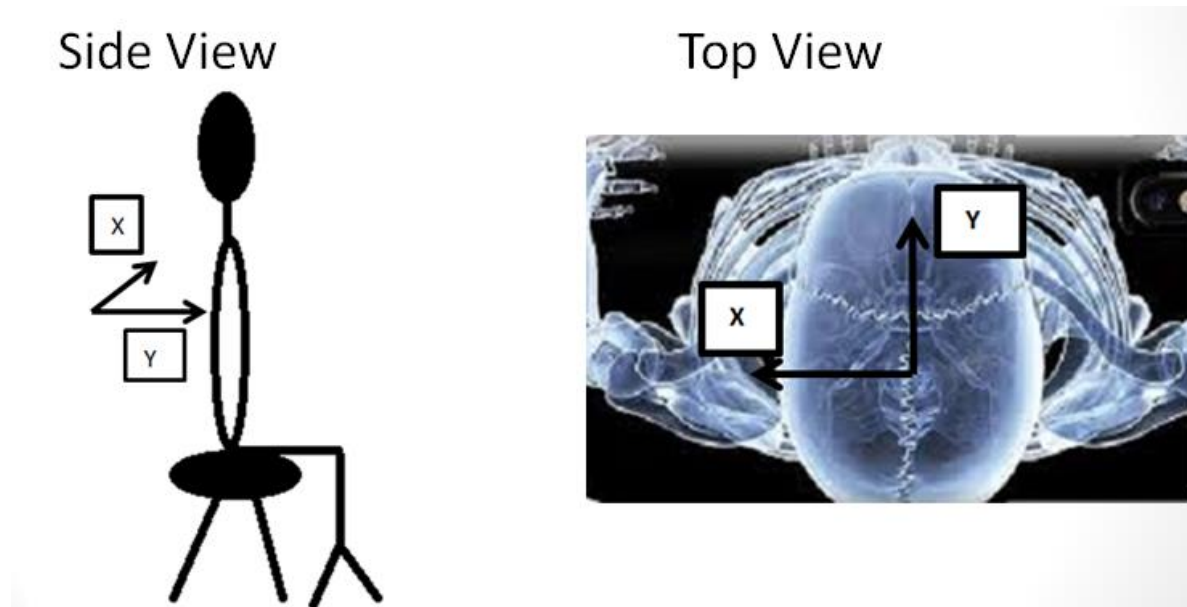


Figure 25 Orientation during Sitting Position

Data was separately recorded in both positions for each subject. The orientation angles were also recorded while the patient was in motion from lying down to sitting in an upright position. Average values and results for cervical, thoracic and lumbar regions in the form of graphs are discussed below.

5.2.1.1 SITTING POSITION

The graphical orientation data is represented separately for each region below along with the average values for sitting position.

5.2.1.1.1 CERVICAL REGION

The mean value from the data set shown in graph below for cervical region is: 60.02 degrees.

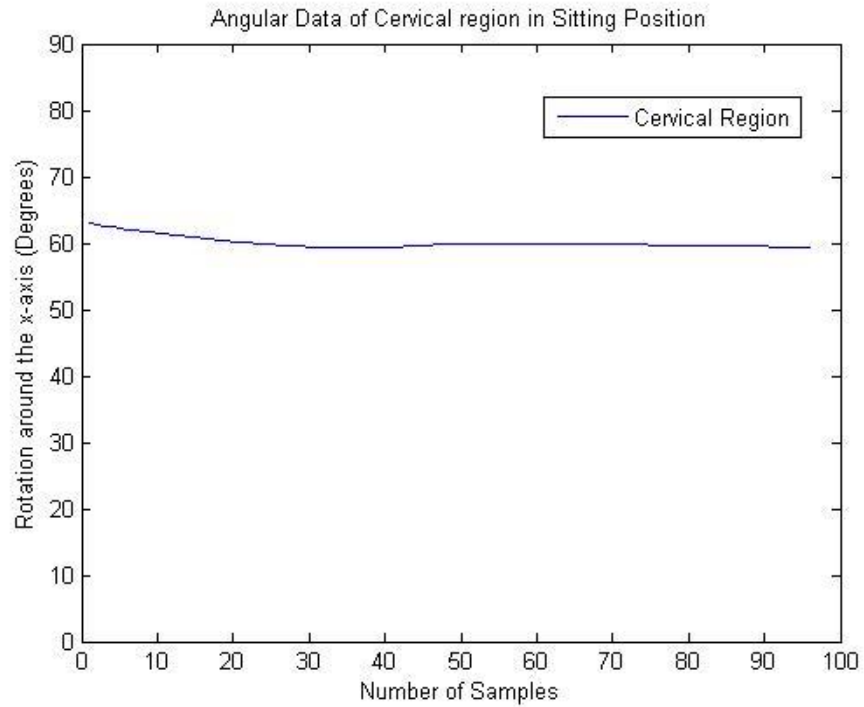


Figure 26 Angular Data of Cervical Region in Sitting Position

5.2.1.1.2 THORACIC REGION

The mean value from the data set shown in graph below for thoracic region is: 67.81 degrees.

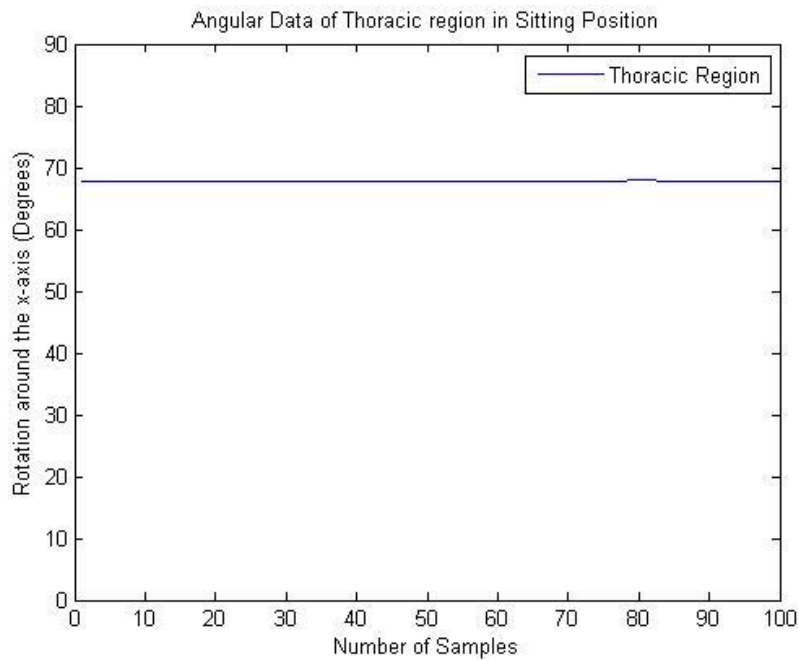


Figure 27 Angular Data of Thoracic Region in Sitting Position

5.2.1.1.3 LUMBAR REGION

The mean value from the data set shown in graph below for lumbar region is: 80.44 degrees.

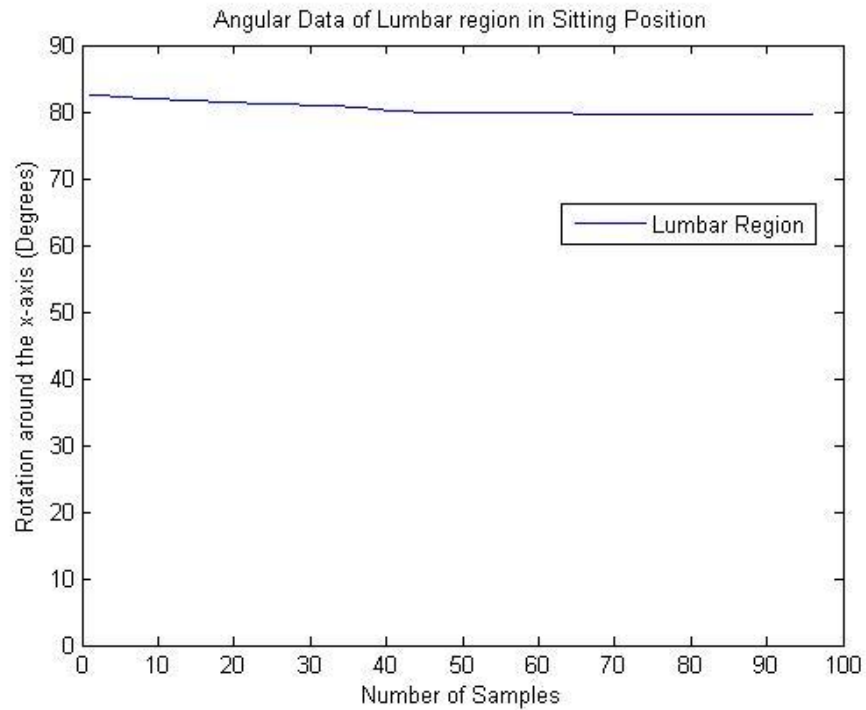
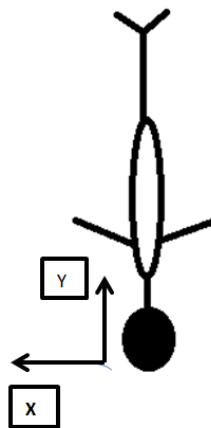


Figure 28 Angular Data of Lumbar Region in Sitting Position

5.2.1.2 LYING DOWN POSITION

The graphical orientation data is represented separately for each region below along with the average values for lying down position. As the figure shows below, the movement is again along the x-axis of the sensor.



5.2.1.2.1 CERVIAL REGION

The mean value from the data set shown in graph below for cervical region is: 13.33 degrees. Considerably lower value as compared to the value of orientation for cervical region in sitting position.

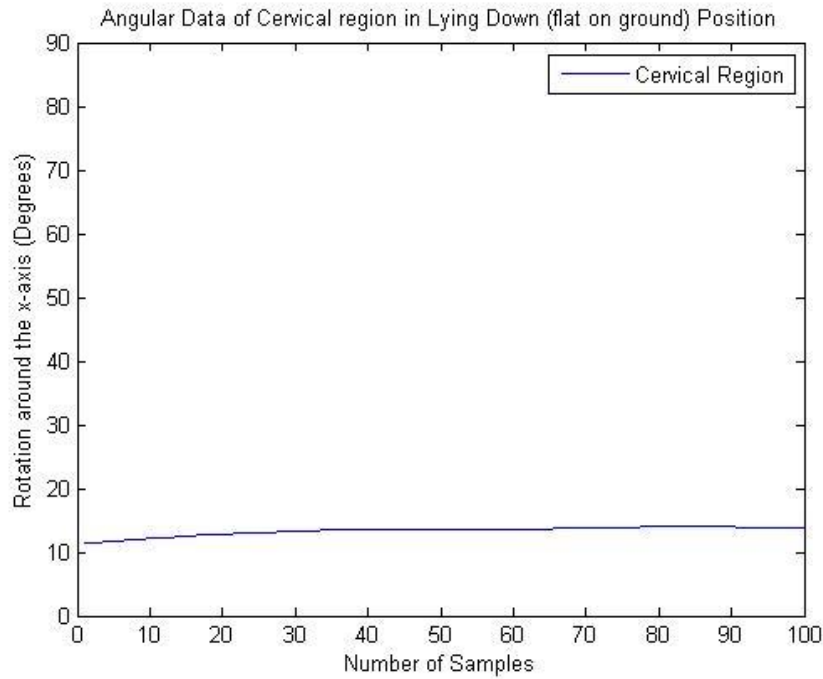


Figure 29 Angular Data of Cervical Region in Lying Down Position

5.2.1.2.2 THORACIC REGION

The mean value from the data set shown in graph below for thoracic region is: -0.96 degrees approximately 0 degrees.

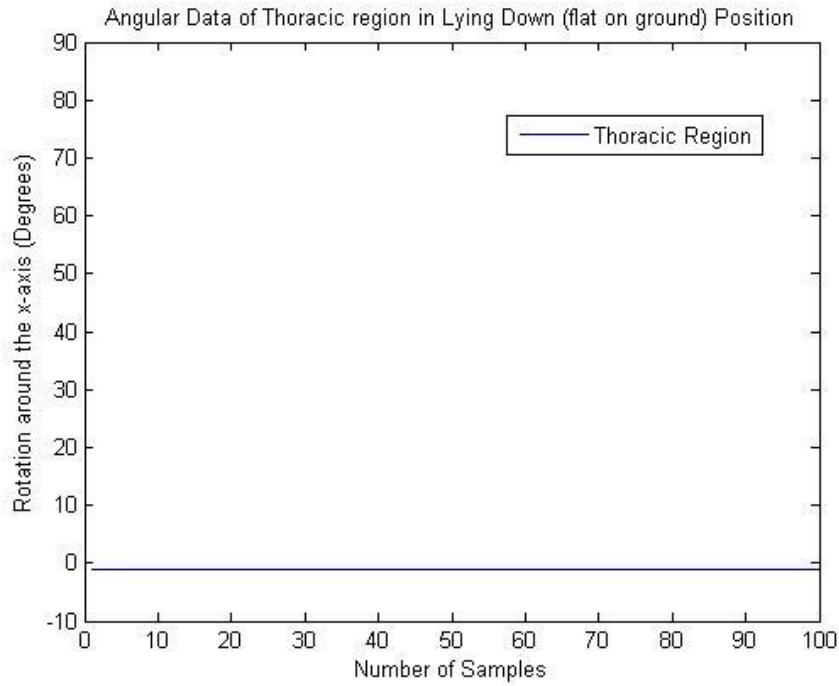


Figure 30 Angular Data of Thoracic Region in Lying Down Position

5.2.1.2.3 LUMBAR REGION

The mean value from the data set shown in graph below for lumbar region is: 13.33 degrees.

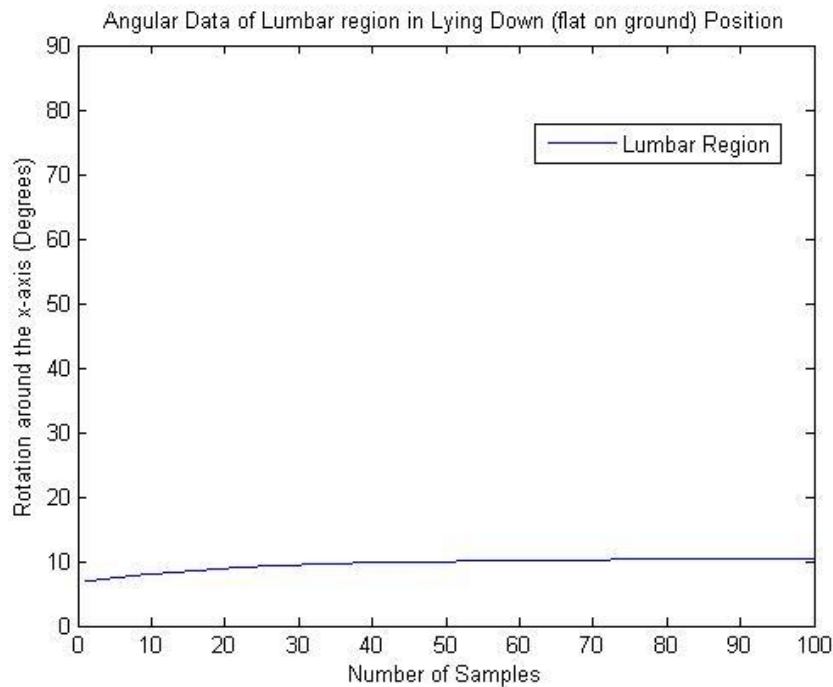


Figure 31 Angular Data of Lumbar Region in Lying Down Position

From the data shown above for both positions, the values of orientation angles go considerably low when the subject is lying down as compared to when the subject is in the sitting position.

This data can be used for two purposes. DAQ system getting these orientation values can be a part of an exoskeleton system so that this is used as an input signal to the control system of the exoskeleton. Patients suffering from Quadriplegia usually need exoskeletons for a 2 DOF motion of just sitting and lying down as not much movement is possible.

Hence, the DAQ system developed in this research and the data collected and analyzed for both sitting and lying down helps to register values for both these movements in general. Also the DAQ system can be separately used to provide real time input signal to the Exoskeleton as well as to differentiate between different types of torso movements.

5.2.2 COMBINED GRAPHS

For easier understanding, combined graphs of all three regions for both sitting and lying down positions are shown below. The graphs represent orientation values for Lumbar region in green, cervical region in red and thoracic region in blue.

5.2.2.1 ORIENTATION DATA OF SPINE DURING SITTING

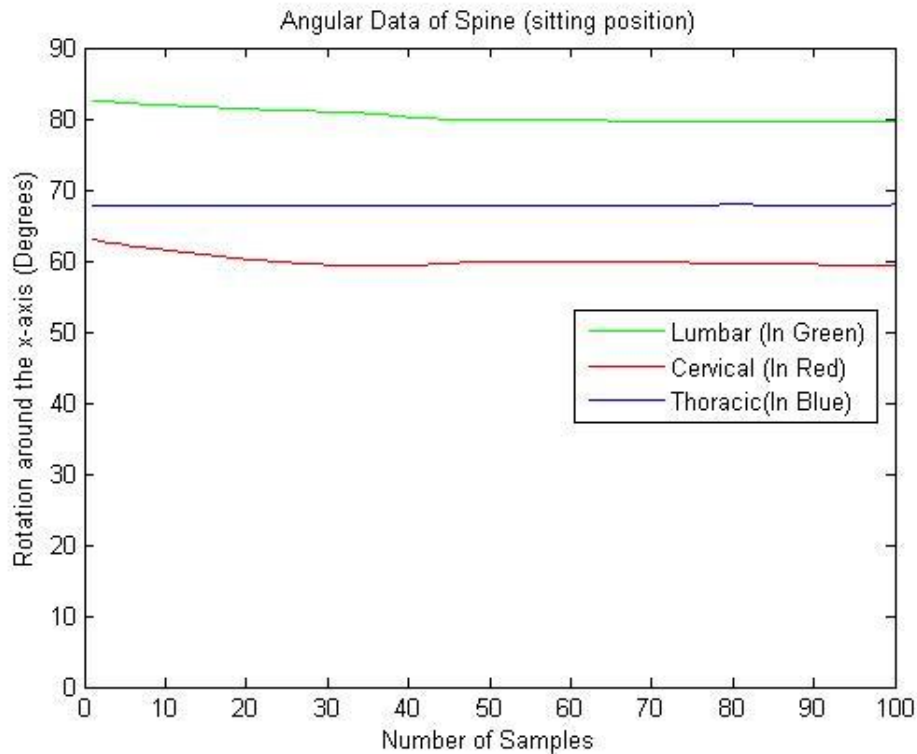


Figure 32 Combined Angular Data of Spine during Sitting

5.2.2.2 ORIENTATION DATA OF SPINE DURING LYING DOWN

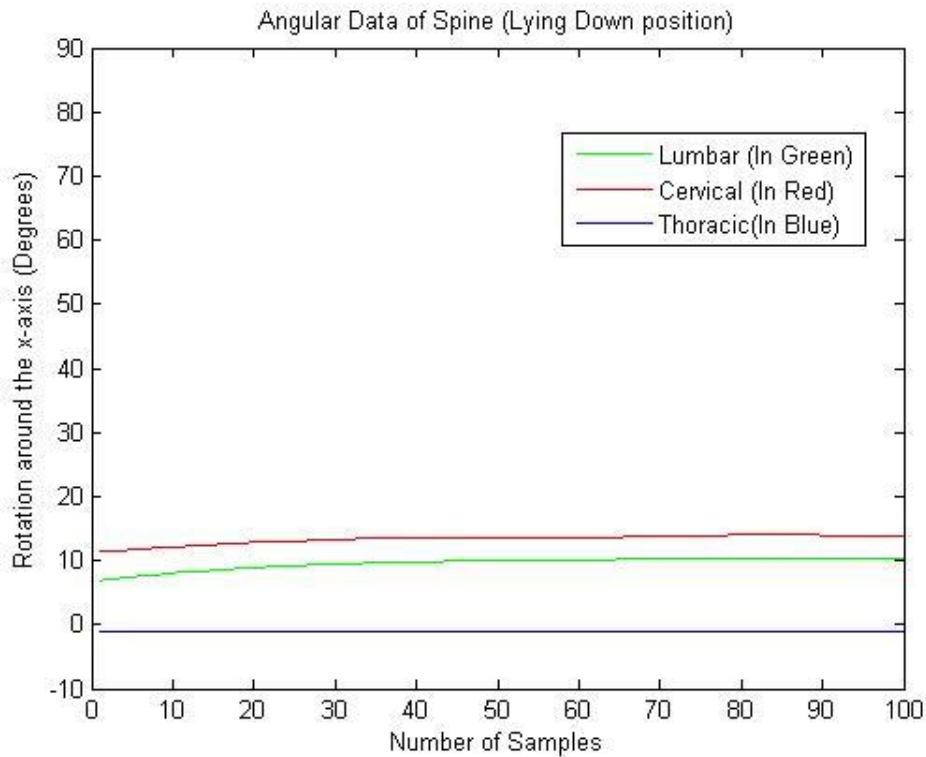


Figure 33 Combined Angular Data of Spine during Lying Down Position

Other experiments included collecting and analyzing data continuously when the patient is moving from lying down to a sitting position. The purpose to do these trials was to establish the fact that the static angles in static positions were the same as when the subject is in motion. The Figure below shows the trend in the values of all three regions when the subject is getting up to sit from a lying down state. The values collected at the start and end of these experiments match the ones that were collected during trials above.

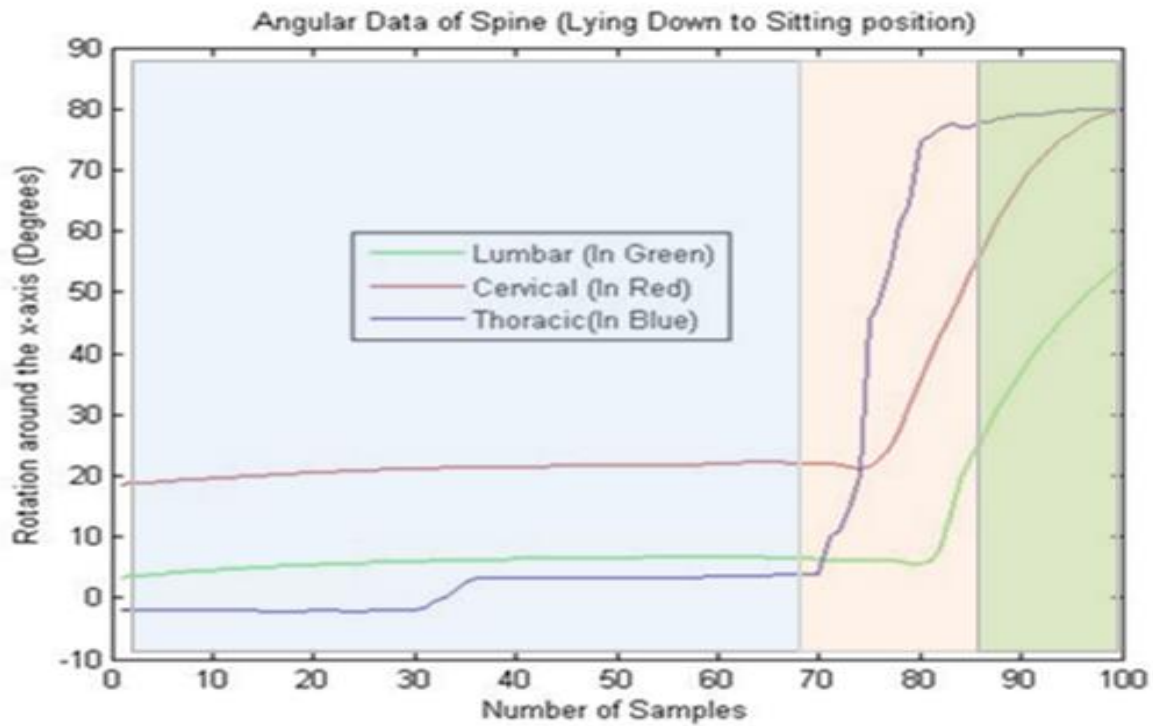


Figure 34 Change in Orientation during Transition from Lying Down to Sitting

5.2.3 COMPARISON OF VALUES WITH MOTION PROCESSING SOFTWARE

The accuracy of values gathered from DAQ system was checked with using motion processing software *Kinovea* (25). The subject was told to sit in a straight sitting position. Motion sensors were attached to the three regions of spinal cord: cervical, thoracic and lumbar. Paper markers were placed on the same spot to mark the regions of sensor placement. Images were taken of the subject's side profile. The image was analyzed for angular data from the three spinal regions with the motion processing software *Kinovea*.

Angles were calculated with respect to the horizontal axis (sagittal plane). Results show that there is not a vast difference between values calculated by the DAQ system and those calculated by using *Kinovea*.

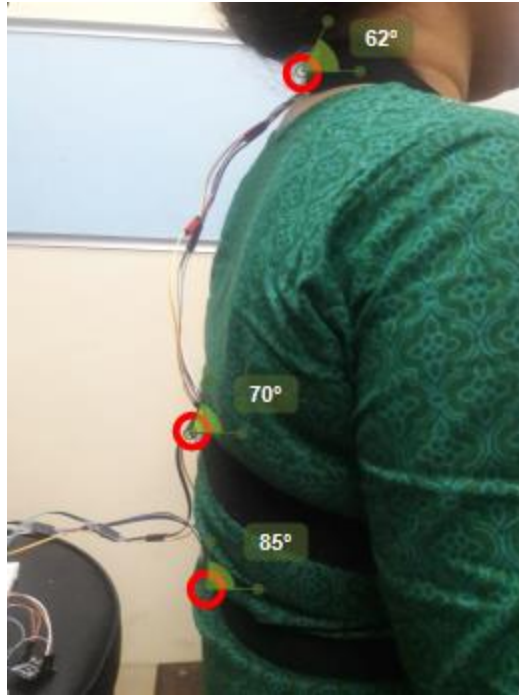


Figure 35 Side Profile of the Subject to analyze with Kinovea

Percentage errors resulting from comparing obtained values from DAQ with those determined by Kinovea are as follows:

- Percentage Error (Cervical Region): 3.2 %
- Percentage Error (Thoracic Region): 4.1 %
- Percentage Error (Lumbar Region): 5.3 %

It should also be noted that errors can result from the subject being non-stationary at an instant of time or the sensor being not attached correctly.

5.2.4 ACCUMULATED SUBJECTS' DATA

An average of three readings from 5 subjects was taken in the same positions. Mean and standard deviation of two positions is shown in the table below:

Table 6 Angular Data of Three Spinal Regions (Mean ± SD)

Positions	Cervical	Thoracic	Lumbar
Sitting	65.13 ± 5.30	71.50 ± 4.59	80.98 ± 5.01
Lying Down	15.39 ± 2.54	-2.96 ± 2.21	5.61 ± 4.65

5.2.5 BIOMECHANICS OF THE WRIST JOINT

A second study was also performed on the Wrist Joint for two pairs of motion. One was Extension and Flexion and the other was Radial and Ulnar Flexion. The purpose was to test the Data Acquisition on one more application of motion differentiation. The joint selected was wrist joint as many applications require the use of a Hand Exoskeleton for amputees and certain movements obtained with the hand need information such as this one.

5.2.5.1 WRIST JOINT

The wrist joint is a synovial joint located in the upper limb and it makes a bridge between the forearm and the hand (26). The wrist joint allows movement along two axes. There are two sets of movements that the wrist joint can perform; extension and flexion plus radial and ulnar flexion. The figure below shows these movements in pictorial form. Extension and flexion is the up and down movement of the hand while radial and ulnar flexion represent the left and right movement of the hand.

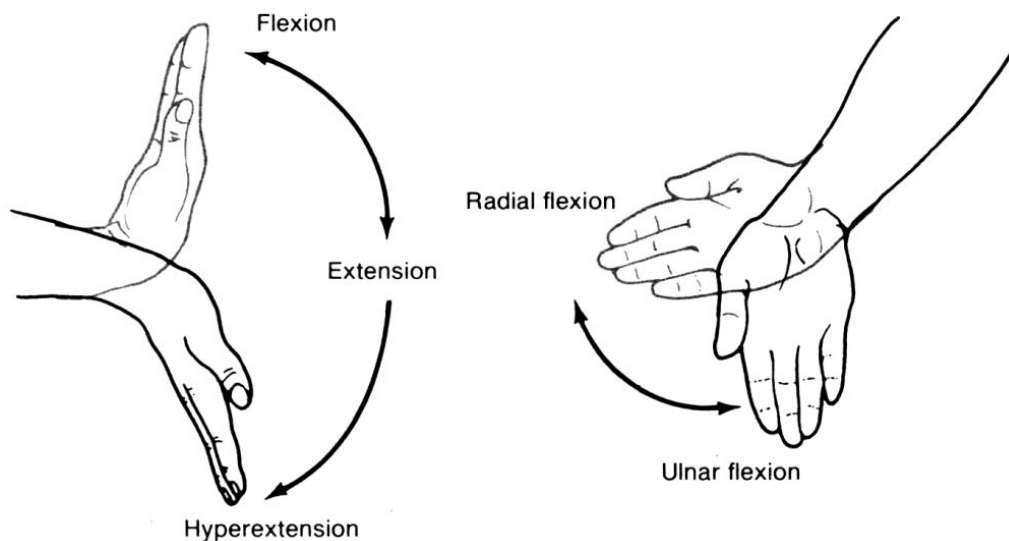


Figure 36 Movements of the Wrist Joint (27)

Figure below shows the setup for testing the data acquisition system on wrist joint. The orientation of the sensor and respective axes are shown in the figure above too. Extension and flexion movements happening around the x-axis of the sensor while the radial and flexion movements are happening around the y-axis of the sensor.

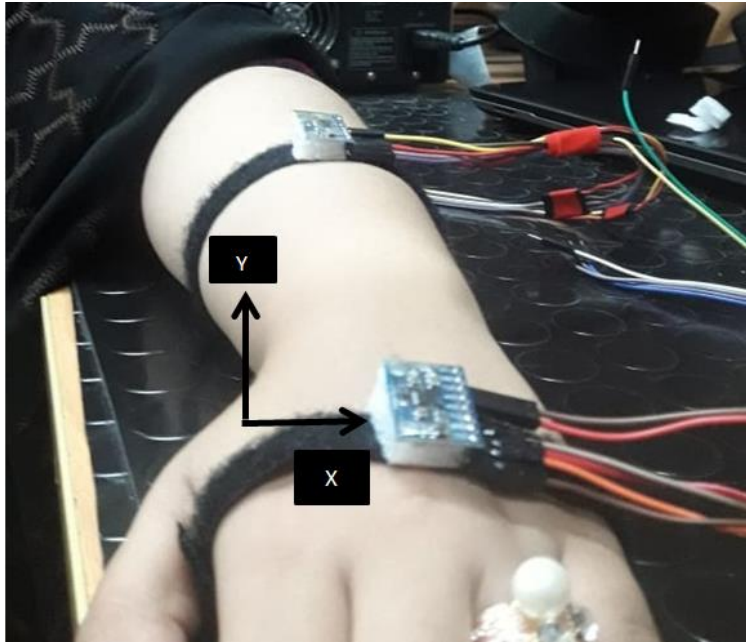


Figure 37 Setup to test DAQ system on Wrist Joint Motion

5.2.5.2 ANALYZING THE DATA & RESULTS

Results are listed for orientation angles obtained by conducting experiments with the DAQ system for extension flexion and radial & ulnar flexion.

5.2.5.2.1 EXTENSION

Mean Value during Extension: 56.53 degrees. Graph shows the areas where the hand was steady and when the wrist joint was moved for extension movement.

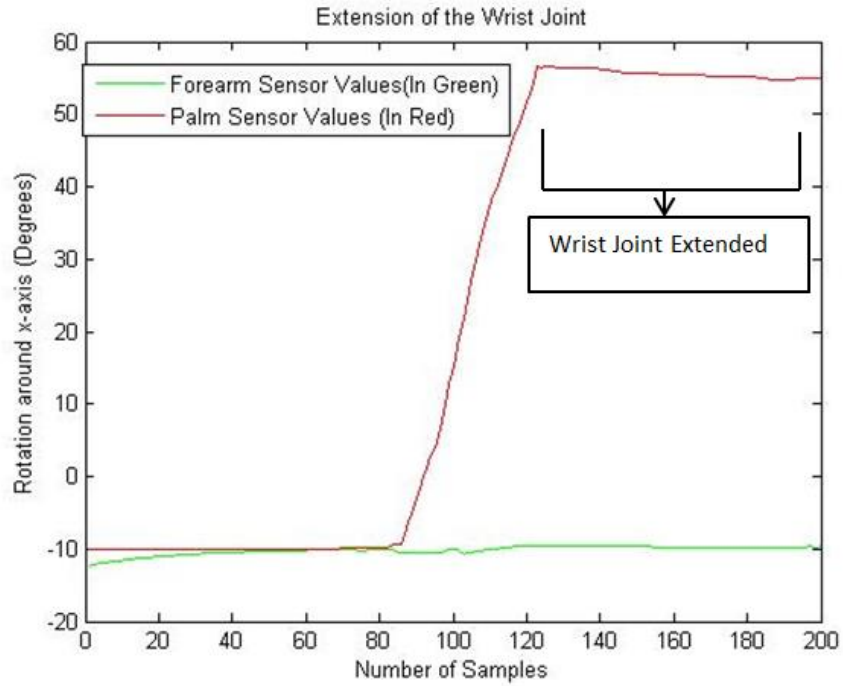


Figure 38 Extension of Wrist Joint

5.2.5.2.2 FLEXION

Mean Value during Flexion: -56.31 degrees

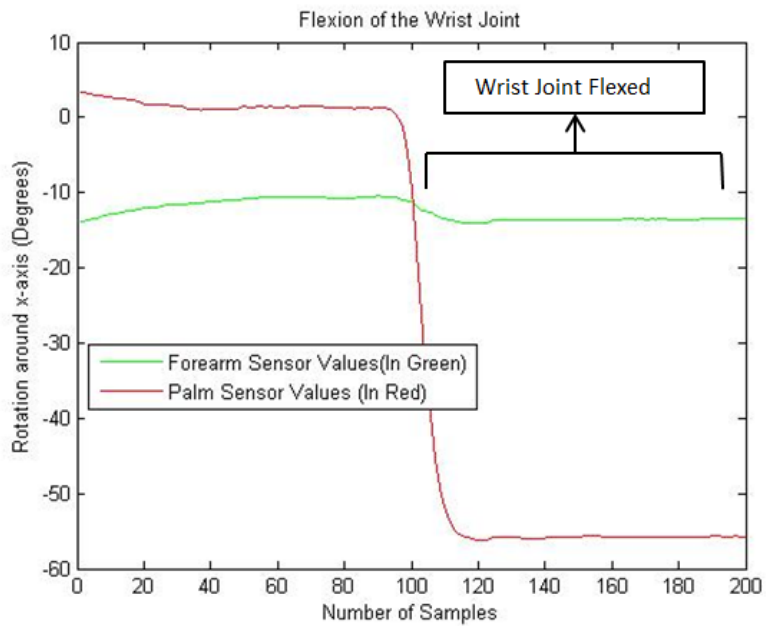


Figure 39 Flexion of the Wrist Joint

5.2.5.2.3 RADIAL FLEXION (LEFT MOVEMENT)

Mean Value during Radial Flexion: -9.91 degrees

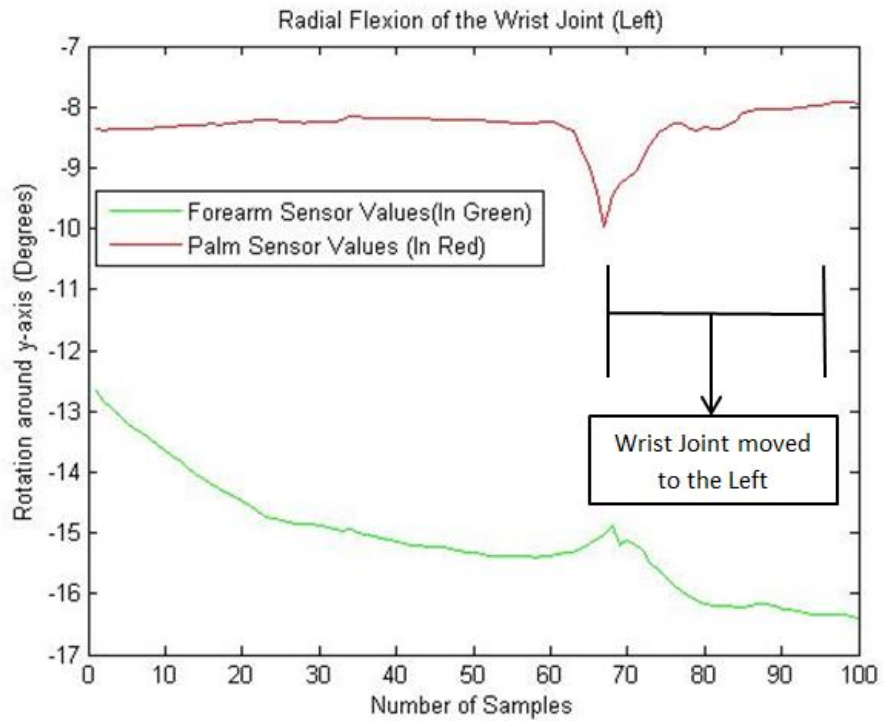


Figure 40 Radial Flexion of the Wrist Joint

5.2.5.2.4 ULNAR FLEXION (RIGHT MOVEMENT)

Mean Value during Ulnar Flexion: -6.880

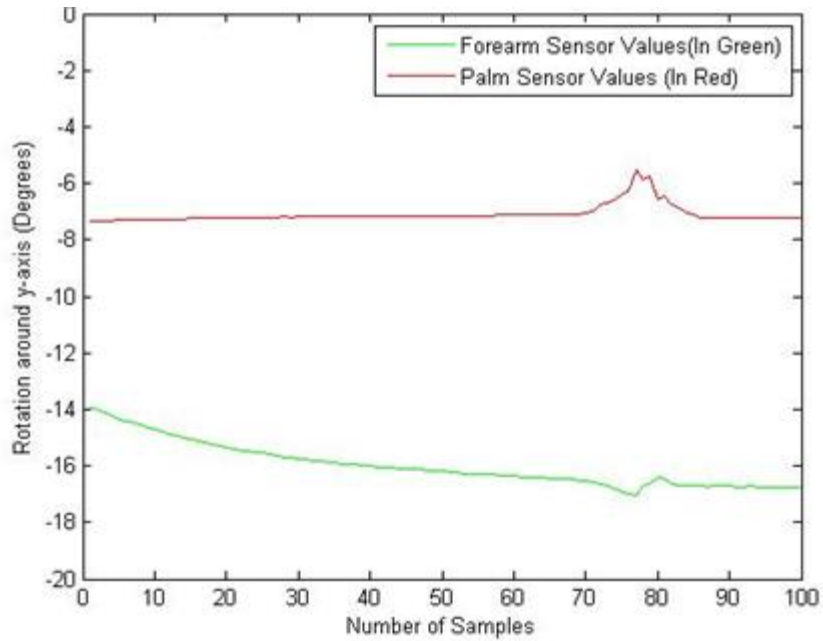


Figure 41 Ulnar Flexion of the Wrist Joint

5.2.5.3 Accumulated Subjects' Data

Data from five subjects was taken for each pair of wrist motion. Then average was taken for each motion performed three times. Mean and standard deviation for the two pairs of motion is shown in the table below:

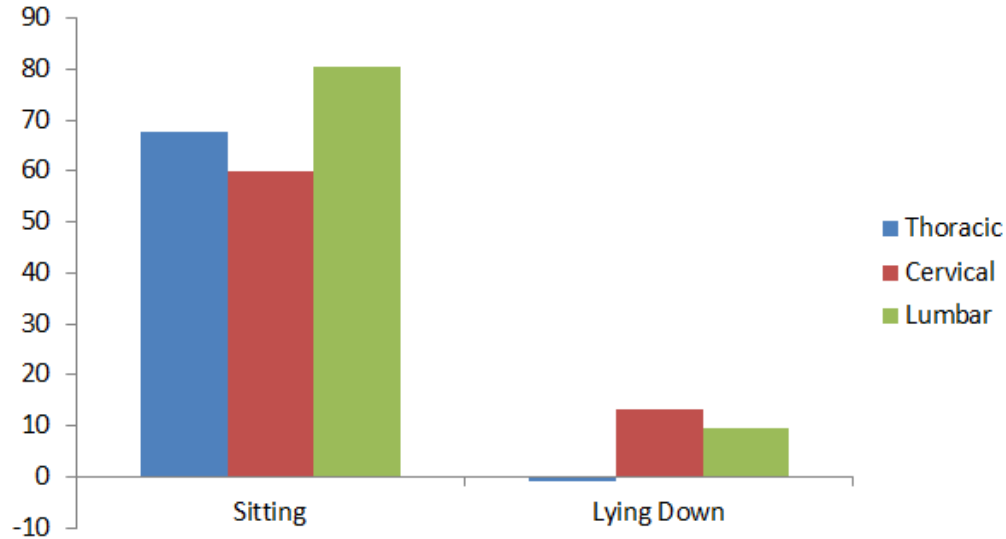
Table 7 Angular Data of Wrist Joint Motion (Mean ± SD)

Extension	Flexion	Radial Flexion	Ulnar Flexion
52.89 ± 2.84	57.13 ± 2.43	-9.91 ± 5.19	-6.23 ± 6.99

CHAPTER 6

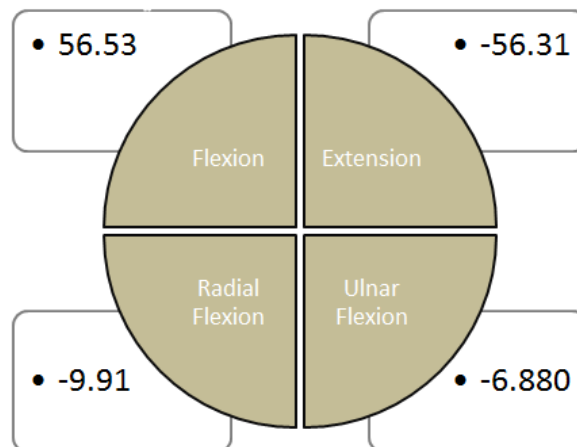
CONCLUSION AND FUTURE PROSPECTS

The comparison of orientation angle values obtained from experiments on spine is shown in the bar graph below. There is a clear and major decrease in orientation angles' values for all three regions. The values range from 55-80 degrees combined for all three regions to 0-15 degrees in sitting to lying down positions respectively.



The values determined with the developed data acquisition system are also compared with motion processing software Kinovea. Results show that the percentage error for each region after being tested and compared with Kinovea is less than 6% for each region.

For the Wrist Joint motion experiments, the comparison of the values obtained is done in the chart below.



The normal range of motion for flexion and extension is 60° while that of radial and ulnar flexion is 20° as is reported in (28), (29), (30) and (31). According to the average values in Table 7 and chart above obtained from DAQ system, there isn't much of a difference in normal range of motion of wrist for these pair of joint motions.

With the help of developed data acquisition system, the type of motion performed by human joints can be determined using only one axis of the Inertial measurement unit. The DAQ system can also be used to provide the input control system to an exoskeleton. The experiments performed and the applications tested in this research make the developed acquisition system capable enough to be used for biomechanical analysis of human body joints, gait analysis and other rehabilitation applications.

6.1 FUTURE PROSPECTS

The data acquisition system developed in this research utilizes one axis to determine the orientation angle information of a moving object and to study biomechanics of joint motion in a single plane. The inertial measurement unit in the DAQ system could be used to make use of all three axes of gyrometer or the accelerometer to get a sense of movement in all three planes of human body and in three dimensions of an object.

Moreover, the applications that the DAQ system was tested on can be extended to perform biomechanics of other joints and using increased the number of sensors to study spinal profile in more detail.

REFERENCES

1. Understanding Spinal Cord Injury. *Shepherd Center*. [Online]
<http://www.spinalinjury101.org/details/levels-of-injury>.
2. **Swift, Timothy Alan**. *Control and trajectory generation of a wearable mobility exoskeleton for spinal cord injury patients*. Mechanical Engineering. Berkeley : University of California, 2011.
3. *Spinal Cord Medicine: Principles and Practice*. **Lin, Vernon**. New York : Demos Medical Publishing, 2002, Journal of the Royal Society of Medicine.
4. *Update on the Pathophysiology and Pathology of Acute Spinal Cord Injury*. **Tator, Charles H.** 4, October 1995, *Brain Pathology*, Vol. 5, pp. 407-413.
5. *Powered exoskeletons for bipedal locomotion after spinal cord injury*. **al, Jose L Contreras-Vidal et. s.l.** : IOP Publishing Ltd, April 2016, *Journal of Neural Engineering*, Vol. 13.
6. Inertial Measurement Unit. *Wikipedia, The Free Encyclopedia*. [Online]
https://en.wikipedia.org/wiki/Inertial_measurement_unit.
7. *Trunk Posture Monitoring With Inertial Sensors*. **Wong, Wai Yin Wong and Man San**. Hong Kong : Springer, 2008, *European Spine Journal*, Vol. 17, pp. 743-753.
8. *Is 'ideal' sitting posture real?: Measurement of spinal curves in four sitting postures*. **Andrew P. Claus, Julie A. Hides, G. Lorimer Moseley, Paul W. Hodges**. s.l. : Elsevier, 2009, *Manual Therapy*, Vol. 14, pp. 404-408.
9. *Dynamic measurement of lumbar curvature using fibre-optic sensors*. **Jonathan M. Williams, Inam Haq, Raymond Y. Lee**. 2010, *Medical Engineering and Physics*, Vol. 32, pp. 1043-1049.
10. *A Mobile Sensing and Imaging System for Real Time Monitoring of Spine Health*. **Noura Farra, Bilal El-Sayed, Nadine Moacdieh, Hazem Hajj, Ziad Hajj, and Rachid Haidar**. s.l. : American Scientific Publishers, 2011, *Journal of Medical Imaging and Health Informatics*, Vol. 1, pp. 1-8.
11. *The Spinal Curvature of Three Different Sitting Positions Analyzed in an Open MRI Scanner*. **Daniel Baumgartner, Roland Zemp, Renate List, Mirjam Stoop, Jaroslav Naxera, Jean Pierre Elsig and Silvio Lorenzetti**. [ed.] F. Galbusera and D. Gastaldi. Zurich, Switzerland : s.n., 2012, *The Scientific World Journal* .
12. *Evaluating the Reproducibility of Motion Analysis Scanning of the Spine During Walking*. **Aaron Gipsman, Lisa Rauschert, Michael Daneshvar, and Patrick Knott**. [ed.] Panagiotis Korovessis. s.l. : Hindawi Publishing Corporation , 17 July, 2014, *Advances in Medicine*, Vol. 2014.
13. 4D Spine and Postural Analysis. *Diers Biomedical Solutions*. [Online]
<https://diers.eu/en/products/spine-posture-analysis/diers-formetric-4d/>.

14. *Design of Information Acquisition and Control System for the Exoskeleton Robot*. **Huan Gou, Jialiu Wang, Hongfang Wu, Chao Wang, Lei Yan, and Jiang Xiao**. [ed.] Xudong Zhu. s.l. : Hindawi Publishing Corporation, 2014, Journal of Electrical and Computer Engineering, Vol. 2014.
15. *Determination of the human spine curve based on laser triangulation*. **Primož Poredoš, Dušan Čelan, Janez Možina and Matija Jezeršek**. 2, s.l. : BioMed Central, 2015, Medical Imaging, Vol. 15.
16. *Using Skin Markers for Spinal Curvature Quantification in Main Thoracic Adolescent Idiopathic Scoliosis: An Explorative Radiographic Study*. **Stefan Schmid, Daniel Studer, Carol-Claudius Hasler, Jacqueline Romkes, William R. Taylor, Reinald Brunner, Silvio Lorenzetti**. [ed.] Han-Chiao Isaac Chen. 8, PLOS One, Vol. 10.
17. *Effect of postural angle on back muscle activities in aging female workers performing computer tasks*. **Nabilla Sofia Mohd Kamil, Siti Zawiah Md Dawal**. s.l. : IPEC Inc, 2015, Journal of Physical Therapy Science, Vol. 27, pp. 1967-1970.
18. 2D wireless Inclinometers. *Noraxon USA*. [Online] <https://www.noraxon.com/our-products/2d-inclinometer/>.
19. **Krystek, Björn**. *Development of a Wearable Electronic Sensor Array and Measuring Unit for Spine and Postural Analysis*. Faculty of Life Sciences, Hamburg University of Applied Sciences. Hamburg : s.n., 2016.
20. Arduino. *Arduino*. [Online] <https://www.arduino.cc/>.
21. *Measurement and Geometric Modelling of Human Spine Posture for Medical Rehabilitation Purposes Using a Wearable Monitoring System Based on Inertial Sensors*. **Gheorghe-Daniel Voinea, Silviu Butnariu and Gheorghe Mogan**. [ed.] Kamiar Aminian. 3, s.l. : MDPI, December 22, 2016, Sensors, Vol. 17.
22. *A Low-Cost, Wearable Opto-Inertial 6-DOF Hand Pose Tracking System for VR*. **Andualem T. Maereg, Emanuele L. Secco, Tayachew F. Agidew, David Reid and Atulya K. Nagar**. 49, s.l. : MDPI, July 28, 2017, Technologies, Vol. 5.
23. **Woodman, Oliver J**. *An introduction to inertial navigation*. University of Cambridge, Computer Laboratory. 2007.
24. SunFounder MPU6050 Module for Arduino and Raspberry Pi, 3-axis Gyroscope and 3-axis Accelerator . *Amazon*. [Online] <https://www.amazon.com/SunFounder-MPU6050-Raspberry-Gyroscope-Accelerator/dp/B0151GI5VI>.
25. *Kinovea*. [Online] <https://www.kinovea.org/>.
26. The Wrist Joint. *Teach Me Anatomy*. [Online] <https://teachmeanatomy.info/upper-limb/joints/wrist-joint/>.

27. The Upper Extremity: The Elbow, Forearm, Wrist, and Hand. [book auth.] Wendi Weimar and Kathryn Luttgens Nancy Hamilton. *Kinesiology: Scientific Basis of human Motion*. 12. s.l. : The McGraw-Hill Companies, 2012, 6.
28. Physical Exam of the Hand. *OrthoBullets*. [Online] <https://www.orthobullets.com/hand/6008/physical-exam-of-the-hand>.
29. [book auth.] Victor and Nordin. *Basic Biomechanics of Musculoskeletal Systems*. s.l. : Lippincott Williams and Wilkins, 2012.
30. *Biokinetic Study of the Wrist Joint*. **Thida Than, Aye Aye San ,Tin Tin Myint**. Malaysia : s.n., 2012, International Journal of Collaborative Research on Internal Medicine & Public Health , Vol. 4.
31. *Range of Joint Motion Evaluation Chart*. s.l., Washington State : Department of Social and Health Services.
32. *A Review on Surface EMG based Control Schemes of Exoskeleton Robot in Stroke Rehabilitation*. **Ram Murat Singh, S. Chatterji, Amod Kumar**. 2013. International Conference on Machine Intelligence Research and Advancement.
33. *Asymmetrical change in the pelvis and the spine during cross-legged sitting postures*. **Soonjae Ahn, Seunghyeon Kim, Sunyoung Kang, Hyeseon Jeon and Youngho Kim**. 11, s.l. : Springer, December, 2013, Journal of Mechanical Science and Technology, Vol. 27, pp. 3427-3432.
34. PlayStation Eye. *WikiPedia*. [Online] https://en.wikipedia.org/wiki/PlayStation_Eye.
35. 9 Degrees of Freedom IMU Breakout - LSM9DS0. *SparkFun*. [Online] STMicroelectronics.

APPENDIX A

ARDUINO CODE:

```
#include "I2Cdev.h"

#include "MPU6050_6Axis_MotionApps20.h"

#if I2CDEV_IMPLEMENTATION == I2CDEV_ARDUINO_WIRE

#include "Wire.h"

#endif

MPU6050 mpu1;

MPU6050 mpu2;

#define TCAADDR 0x70

#define OUTPUT_READABLE_YAWPITCHROLL

#define INTERRUPT_PIN_1 15 // use pin 2 on Arduino Uno & Mega while 15 on esp8266 because
gpio15 is interrupt pin which is D8 on esp

#define INTERRUPT_PIN_2 13 //D7

#define LED_PIN 13 // (Arduino is 13, Teensy is 11, Teensy++ is 6)

bool blinkState = false;

bool dmpReady1 = false; // set true if DMP init was successful

uint8_t mpuIntStatus1; // holds actual interrupt status byte from MPU

uint8_t devStatus1; // return status after each device operation (0 = success, !0 = error)

uint16_t packetSize1; // expected DMP packet size (default is 42 bytes)

uint16_t fifoCount1; // count of all bytes currently in FIFO

uint8_t fifoBuffer1[64]; // FIFO storage buffer

bool dmpReady2 = false; // set true if DMP init was successful

uint8_t mpuIntStatus2; // holds actual interrupt status byte from MPU

uint8_t devStatus2; // return status after each device operation (0 = success, !0 = error)
```

```

uint16_t packetSize2; // expected DMP packet size (default is 42 bytes)
uint16_t fifoCount2; // count of all bytes currently in FIFO
uint8_t fifoBuffer2[64]; // FIFO storage buffer

Quaternion q1; // [w, x, y, z] quaternion container
VectorInt16 aa1; // [x, y, z] accel sensor measurements
VectorInt16 aaReal1; // [x, y, z] gravity-free accel sensor measurements
VectorInt16 aaWorld1; // [x, y, z] world-frame accel sensor measurements
VectorFloat gravity1; // [x, y, z]
float euler1[3]; // [psi, theta, phi]
float ypr1[3];

Quaternion q2; // [w, x, y, z] quaternion container
VectorInt16 aa2; // [x, y, z] accel sensor measurements
VectorInt16 aaReal2; // [x, y, z] gravity-free accel sensor measurements
VectorInt16 aaWorld2; // [x, y, z] world-frame accel sensor measurements
VectorFloat gravity2; // [x, y, z]
float euler2[3];
float ypr2[3]; // [yaw, pitch, roll] yaw/pitch/roll container and gravity vector
volatile bool mpuInterrupt1 = false; // indicates whether MPU interrupt pin has gone high
void dmpDataReady1() {
    mpuInterrupt1 = true;
}

volatile bool mpuInterrupt2 = false; // indicates whether MPU interrupt pin has gone high
void dmpDataReady2() {
    mpuInterrupt2 = true;
}

void tcselect(uint8_t i) {
    if (i > 7) return;

```

```

Wire.beginTransmission(TCAADDR);

Wire.write(1 << i);

Wire.endTransmission();

}

void setup() {

    // join I2C bus (I2Cdev library doesn't do this automatically)

    #if I2CDEV_IMPLEMENTATION == I2CDEV_ARDUINO_WIRE

        Wire.begin();

        Wire.setClock(400000); // 400kHz I2C clock. Comment this line if having compilation difficulties

    #elif I2CDEV_IMPLEMENTATION == I2CDEV_BUILTIN_FASTWIRE

        Fastwire::setup(400, true);

    #endif

    Serial.begin(115200);

    while (!Serial); // wait for Leonardo enumeration, others continue immediately

    tcselect(2);

    mpu1.initialize();

    pinMode(INTERRUPT_PIN_1, INPUT);

    mpu1.setFullScaleAccelRange(MPU6050_ACCEL_FS_16);
    mpu1.setFullScaleGyroRange(MPU6050_GYRO_FS_2000);
    mpu1.setDLPFMode(MPU6050_DLPF_BW_42);

    tcselect(7);

    mpu2.initialize();

    pinMode(INTERRUPT_PIN_2, INPUT);

    mpu2.setFullScaleAccelRange(MPU6050_ACCEL_FS_16);
    mpu2.setFullScaleGyroRange(MPU6050_GYRO_FS_2000);
    mpu2.setDLPFMode(MPU6050_DLPF_BW_42);

```

```

tcselect(2);

Serial.println(mpu1.testConnection() ? F("MPU6050 connection successful") : F("MPU6050
connection failed"));

tcselect(7);

Serial.println(mpu2.testConnection() ? F("MPU6050 connection successful") : F("MPU6050
connection failed"));

while (Serial.available() && Serial.read()); // empty buffer
while (!Serial.available()); // wait for data
while (Serial.available() && Serial.read()); // empty buffer again
tcselect(2);

devStatus1 = mpu1.dmpInitialize();

tcselect(7);

devStatus2 = mpu2.dmpInitialize();

tcselect(2);

mpu1.setXGyroOffset(70);
mpu1.setYGyroOffset(111);
mpu1.setZGyroOffset(54);
mpu1.setZAccelOffset(1514); // 1688 factory default for my test chip
tcselect(7);

mpu2.setXGyroOffset(70);
mpu2.setYGyroOffset(111);
mpu2.setZGyroOffset(54);
mpu2.setZAccelOffset(1514);

tcselect(2);

if (devStatus1 == 0) {
    mpu1.setDMPEnabled(true);
    attachInterrupt(digitalPinToInterrupt(INTERRUPT_PIN_1), dmpDataReady1, RISING);
    mpuIntStatus1 = mpu1.getIntStatus();

```

```

    dmpReady1 = true;
    packetSize1 = mpu1.dmpGetFIFOPageSize();
} else {
    Serial.print(F("DMP Initialization failed (code ");
    Serial.print(devStatus1);
    Serial.println(F(")"));
}
tcselect(7);
if (devStatus2 == 0)
    mpu2.setDMPEnabled(true);
    attachInterrupt(digitalPinToInterrupt(INTERRUPT_PIN_2), dmpDataReady2, RISING);
    mpuIntStatus2 = mpu2.getIntStatus();
    dmpReady2 = true;
    packetSize2 = mpu2.dmpGetFIFOPageSize();
} else {
    Serial.print(F("DMP Initialization failed (code ");
    Serial.print(devStatus2);
    Serial.println(F(")"));
}
}
String jsonEncodeValue(String key, float keyVal){
    return "\"" + key + "\": " + String(keyVal) + "\"";
}
String assembleJson(String keysAndVals){
    return "{" + keysAndVals + "}";
}
void loop() {
tcselect(2);
    if (!dmpReady1) return;

```

```

while (!mpuInterrupt1 && fifoCount1 < packetSize1) {
}
mpuInterrupt1 = false;
mpuIntStatus1 = mpu1.getIntStatus();
fifoCount1 = mpu1.getFIFOCount();
if ((mpuIntStatus1 & 0x10) || fifoCount1 == 1024) {
    mpu1.resetFIFO();
} else if (mpuIntStatus1 & 0x02) {
    while (fifoCount1 < packetSize1) fifoCount1 = mpu1.getFIFOCount();
    tcselect(2);
    mpu1.getFIFOBytes(fifoBuffer1, packetSize1);
    fifoCount1 -= packetSize1;

    mpu1.dmpGetQuaternion(&q1, fifoBuffer1);
    mpu1.dmpGetGravity(&gravity1, &q1);
    mpu1.dmpGetYawPitchRoll(ypr1, &q1, &gravity1);

    blinkState = !blinkState;
    digitalWrite(LED_PIN, blinkState);
}}
}

```


APPENDIX B

MATLAB CODE:

```
com=serial('COM4','Baudrate',115200);
fopen(com);
n=10000; %record up to a 500 time instants
Y1=zeros(1,n);
P1=Y1;
R1=Y1;
Y2=zeros(1,n);
P2=Y2;
R2=Y2;

fprintf(com,'A');

for i=1:1:n

    keyVals=fscanf(com,'%s');
    loadjson(keyVals);
    R1=ans.r1;
    P1=ans.p1;
    Y1=ans.y1;

    R2=ans.r2;
    P2=ans.p2;
    Y2=ans.y2;

    X=[R1 P1 Y1];
    Z=[R2 P2 Y2];
    R=R1-R2;
    P=P1-P2;
    Y=Y1-Y2;
    C=[R P Y];
    [x,y,z] = sphere ;h = surf(x,y,z);axis('square');
    title('orientation');
    xlabel('x'); ylabel('y'); zlabel('z');
    %Rotate Object
    rotate(h,[1,0,0], R)
    rotate(h,[0,1,0], P)
    rotate(h,[0,0,1], Y)
    view(3);
    drawnow
end
fclose(com);
delete(com);
clear com;
delete(instrfindall);
```

